
Article:
Georgieva, MN, Little, CTS orcid.org/0000-0002-1917-4460, Maslennikov, VV et al. (3 more authors) (2021) The history of life at hydrothermal vents. Earth-Science Reviews, 217. 103602. ISSN 0012-8252

https://doi.org/10.1016/j.earscirev.2021.103602

The history of life at hydrothermal vents

Magdalena N. Georgieva[1], Crispin T. S. Little[1,2], Valeriy V. Maslennikov[3], Adrian G. Glover[1], Nuriya R. Ayupova[3], Richard J. Herrington[4]

[1]Life Sciences Department, Natural History Museum, London, United Kingdom

[2]School of Earth and Environment, University of Leeds, Leeds, United Kingdom

[3]South Urals Federal Research Center of Mineralogy and Geoecology, Urals Branch, Russian Academy of Sciences, Miass, Russia

[4]Earth Sciences Department, Natural History Museum, London, United Kingdom

Correspondence

Magdalena N. Georgieva

Email: magdalena.n.georgieva@gmail.com

Address: Life Sciences Department, Natural History Museum, London, United Kingdom

ORCIDs

MNG, 0000-0002-1129-0571

CTSL, 0000-0002-1917-4460

VVM, 0000-0002-1999-2324

AGG, 0000-0002-9489-074X

NRA, 0000-0003-0792-1876

RJH, 0000-0003-1576-8242

Keywords

evolution; chemosynthesis; deep sea; pyrite preservation; cold seep; volcanogenic massive sulfide

Abstract

Hydrothermal vents are among the most fascinating environments that exist within the modern oceans, being home to highly productive communities of specially-adapted fauna, supported by chemical energy emanating from the Earth's subsurface. As hydrothermal vents have been a feature our planet since the Hadean, their history is intricately weaved into that of life on Earth. Despite an overall scant fossil record due to the improbabilities of preservation of vent deposits and organisms, recent fossil findings from ancient vent environments, accompanied by molecular data as well as fossils from ecologically-similar environments, have yielded invaluable new insights into the history of life at hydrothermal vents. Fossils from hydrothermal vents are among the earliest contenders for direct evidence of life on Earth, while a range of additional fossil finds indicate that vent habitats were readily exploited by microbes during the Precambrian. The first metazoans possibly appeared within vents during the Cambrian, and by the Ordovician-Silurian, hydrothermal vents in the deep ocean were colonised by mollusc, brachiopod and tubeworm taxa whose large abundances and sizes suggest these early animals were well-adapted to this setting. A transition in vent community composition occurred during the Mesozoic, as modern vent faunas began to occupy these environments and replace Paleozoic taxa. Molecular evidence indicates that many additional taxa radiated within vents during the Cenozoic, demonstrating that throughout Earth history, organisms were repeatedly able to overcome the challenges of adapting to the harsh conditions at vents to exploit their productivity. Targeting ancient vent deposits that have undergone low degrees of diagenetic or metamorphic change during mining-related exposure has great potential to provide further insights into the vent fossil record and fill existing gaps in knowledge.

1 Introduction

Hydrothermal vents are one of the earliest types of environment to have existed on Earth, having been a feature of our planet and the world oceans since the Hadean, 4.6-4.0 billion years ago (Ga) (Russell and Hall, 1997; Martin et al., 2008). They are characterized by the ejection of hot, mineral- and chemical-rich fluids from the seafloor, typically at bathyal depths. As well as being important geological

structures that concentrate minerals of economic significance, they support remarkable biological communities with rare and endemic species specially adapted to the conditions that vents present. Vent environments are intimately connected to the history of life, as they are deemed a highly probable setting for its origination (Reysenbach and Cady, 2001; Martin et al., 2008; Weiss et al., 2016), and have a fossil history that possibly extends to the first direct evidence of life on Earth (Dodd et al., 2017), demonstrating their importance as biological habitats throughout Earth history (Little et al., 1998). Since the fossil record of hydrothermal vents was last reviewed (Little et al., 1998; Campbell, 2006), numerous new fossil finds have been discovered, particularly from the Ural Mountains (Maslennikov et al., 2016, 2017; Ayupova et al., 2017), while molecular phylogenetics has illuminated the evolutionary histories of vent fauna absent from the fossil record. This review sets out to provide an overview of the history of life within marine vent environments that weaves together data from diverse sources, to document the role of hydrothermal vents in shaping biotic evolution on our planet.

1.1 Geology and chemistry of hydrothermal vents

Hydrothermal vents on the modern deep-seafloor were first discovered by deep towed cameras in 1976 and subsequently visited for the first time by submersible in 1977 (Lonsdale, 1977; Corliss et al., 1979), after having been predicted to exist through global heat budget calculations (Lalou, 1991). While the vents themselves were expected, that they would be populated by lush biological communities was not anticipated. The physico-chemical conditions that vents provide are central to their ability to sustain highly productive ecosystems. Hydrothermal vents can develop wherever a heat source comes into close contact with a crustal fluid system, resulting in the convective flow of fluid to the seafloor. The term 'hydrothermal vents' is largely applied to marine hydrothermal systems, which are the focus of this review, however analogous systems can also form in freshwater bodies (such as Lake Baikal) or in the terrestrial realm, where they are known as hot springs. In the marine environment, hydrothermal vents are predominantly associated with the deep ocean, where they arise in relation to seafloor extension at a range of tectonic sites (Fig. 1A). However, hydrothermal vents are also commonly found in association with active volcanoes, seamounts, and continental rifts, and

can thus occur at almost any depth. The majority of known hydrothermal vents occur along the axis of mid-ocean ridges (65%), but vents are also common along volcanic arc (12%) as well as within back-arc basins (22%) (Fig. 1A) (Hannington et al., 2011). Within extensional settings, spreading of the seafloor results in the upwelling of magma below the crust, as well in cracks and fissures as oceanic plates are stretched. This increased porosity enables seawater to percolate deep into oceanic crust, where it is heated, reacts with rocks in the subsurface, and is subsequently convected upwards towards the seafloor, erupting as a hydrothermal vent.

By the time hydrothermal fluids reach the seafloor, they can have temperatures of around 350-407°C (Koschinsky et al., 2008), have interacted with rocks in the sub-seafloor, and represent near-neutral, complex mixtures laden with chemically-reduced dissolved minerals (typically iron, zinc and copper sulfides, silica, anhydrite, barite) and gases (hydrogen sulfide, hydrogen, methane). The interaction of escaping hydrothermal fluids with cool seawater at the seabed usually results in mineral precipitation, producing characteristic chimney structures (Fig. 2A, C) that exhibit zonation relating to the conditions under which various mineral phases precipitate, particularly temperature. However, the morphology of hydrothermal vent deposits can be highly variable depending on the rate of seafloor spreading, fluid flow dynamics, and internal plumbing conditions and duration of venting. Therefore, hydrothermal vent precipitates can also manifest as non-chimney structures, such as complex sulfide mounds (Van Dover, 2000).

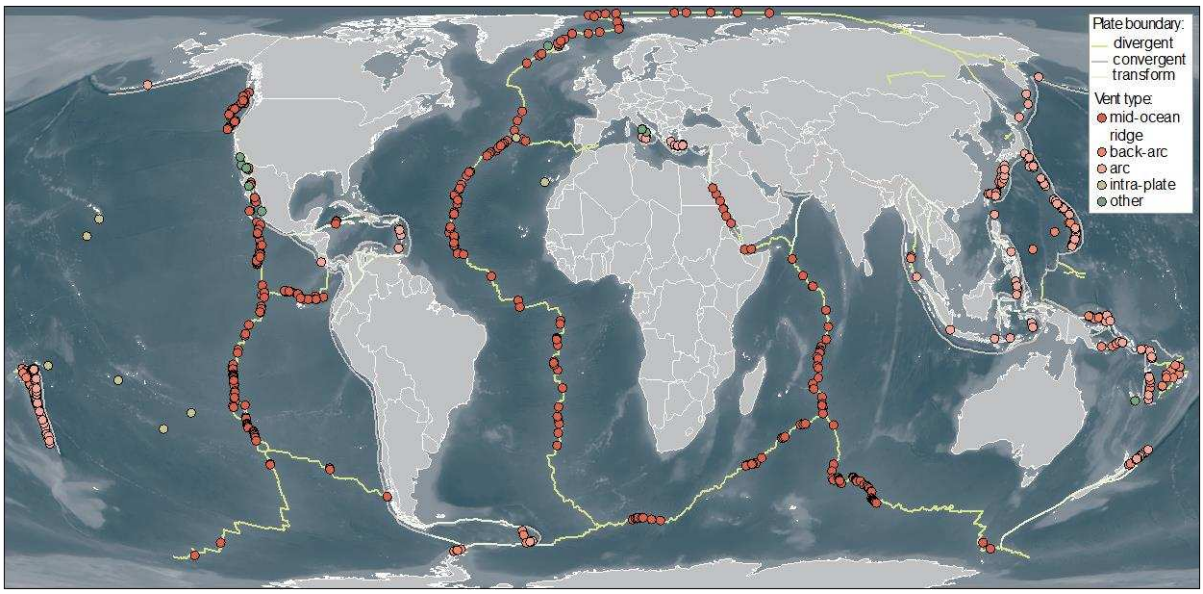

Figure 1. Locations of hydrothermal vents today (confirmed and inferred) categorised by type. Source: InterRidge Vent Database v. 3.3.

Hydrothermal venting may also occur through sediments, whereby vent fluids mix with seawater below the seabed, sometimes resulting in vent fluids rich in hydrocarbons and the deposition of minerals at depth within the sediment (Von Damm et al., 1985). In addition, sedimentary-chemical deposits variously termed metalliferous mudstones, exhalites, iron formations, jaspers (hematitic chert), gossanites, or hydrothermal mudstones, form at the peripheries of hydrothermal vents as a result of hydrothermal plume fallout, or the oxidation of existing chimney structures (Haymon and Kastner, 1981; Gurvich, 2006). Some of these are direct precipitates from low temperature, iron-rich, but sulfide-poor vent fluids. These deposits can be layered, form small domes, and/or small chimney structures, especially where there has been some associated silica precipitation (Sun et al., 2015).

Because of the action of hydrothermal vents to concentrate and precipitate minerals of economic importance such as copper, lead, silver, gold, and zinc (Galley et al., 2007), they are of interest for mineral exploitation. Hydrothermal vent deposits on the modern seafloor are also referred to as seafloor massive sulfides (SMS) especially in relation to mineral extraction activities (Hannington et al., 2011). The extraction of SMS from the modern seafloor is largely still in its infancy due to the challenges of mining operations at depths of over 2,000 m below sea level, and compared to ancient

vent deposits, appear to contain much smaller mineral reserves (Petersen et al., 2016). Research into where large SMS reserves may be forming is the subject of intense scientific investigation (German et al., 2016).

1.2 Biology of modern hydrothermal vent environments

The highly unusual fauna that astounded the first explorers of deep-sea hydrothermal vents in 1977 prompted the establishment of a completely new branch of deep-sea biology. The deep sea is generally a resource-poor environment sustained by the continuous sinking of nutrients from surface waters, resulting in low-productivity but diverse benthic communities dominated by deposit- and filter-feeders. In contrast, hydrothermal vent communities are comprised of generally high abundances of few animal species which are sustained by chemosynthesis, which is the harnessing of energy through the use of reduced chemical compounds to fix carbon. Chemosynthesis at deep-sea vents is a process carried out by microbes capable of chemolithotrophy, of which bacteria of the phyla Proteobacteria and Campylobacterota have been shown to be particularly important (Dubilier et al., 2008; Sogin et al., 2020). These bacteria use the reduced chemical species that are abundant in vent fluids, such as hydrogen sulfide, as electron donors to convert carbon dioxide into organic compounds. The dominant metazoans found within modern vent environments form symbiotic associations with chemolithotrophic bacteria, which may be incorporated into animal tissues (endosymbiosis) or attached to animal surfaces (ectosymbiosis). The establishment of such symbioses is deemed one of the most important adaptations that enables metazoans to colonise hydrothermal vents, with these intimate associations being crucial to the ability of vent-specialist taxa to sustain high abundances within vent environments.

Annelid tubeworms of the family Siboglinidae, bathymodiolin mussels, vesicomyid clams, provannid gastropods, alvinocaridid shrimp, eolepadid barnacles and *Kiwa* anomuran crabs (Fig. 2A-C) are among the most prominent occupants of present-day vent environments (Desbruyères et al., 2006), while a host of heterotrophic taxa are usually found living among vent specialists. Some of the animals

which are highly successful at vents can also be found within other deep-sea chemosynthetic environments such as cold seeps and organic falls, and are deemed to have complex evolutionary trajectories that likely involve several chemosynthetic habitat types (Hilário et al., 2011; Smith et al., 2015; Kiel, 2016).

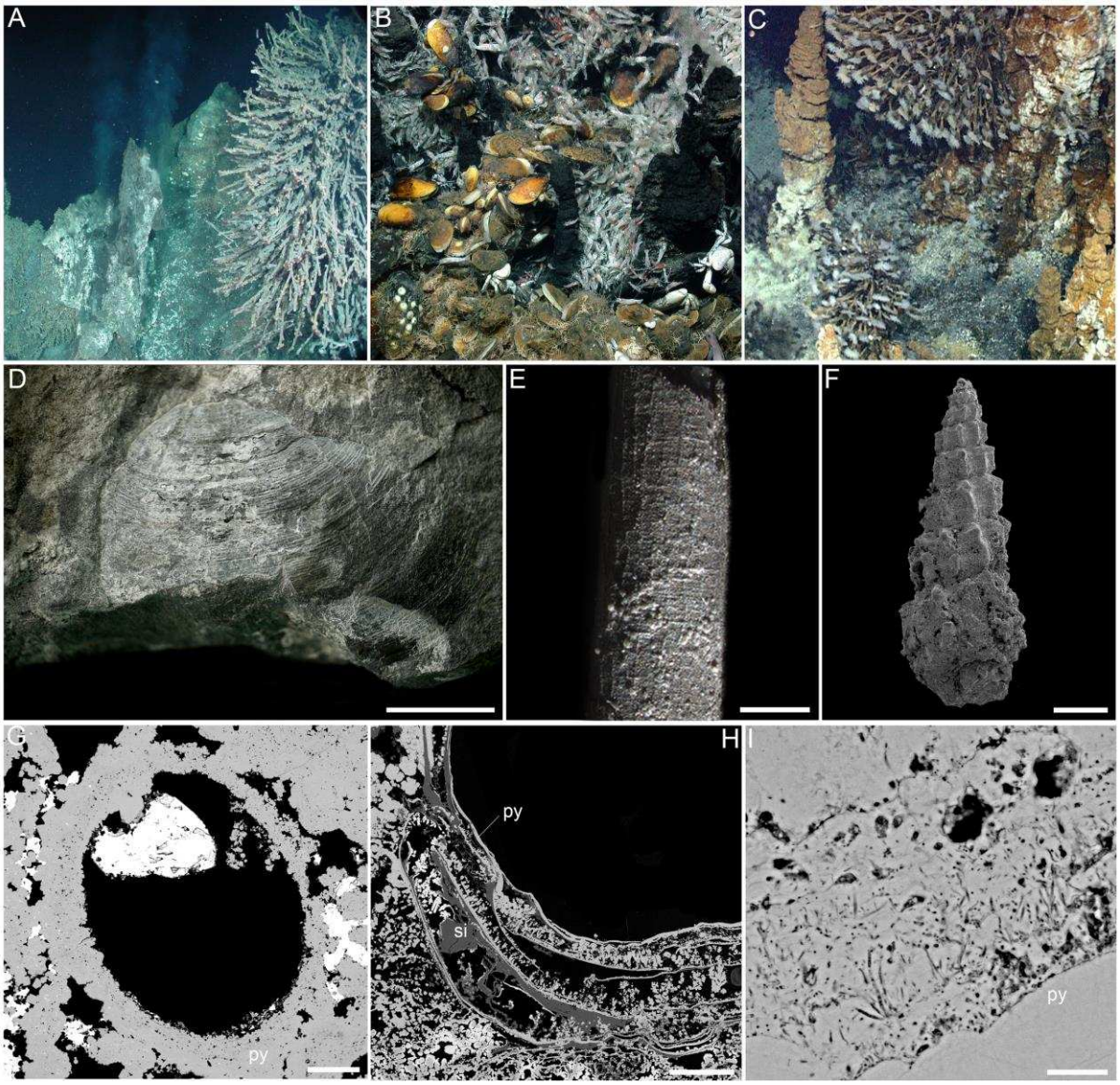

Figure 2. Modern and ancient vent fauna, and its preservation. **A**, siboglinid tubeworms (*Ridgeia piscesae*) at the Magic Mountain vent site, Explorer Ridge, NE Pacific. Image credit: NOAA. **B**, bathymodiolin mussels and alvinocaridid shrimps, Mid-Ocean Ridge hydrothermal vents. Image credit: MARUM. **C**, eolepadid barnacles at the Kawio Barat volcano vent site. Image credit: NOAA Okeanos Explorer. **D**, the lingulate brachiopod *Pyrodiscus lorrainae* from the Ordovician-Silurian Yaman Kasy deposit, scale bar is 20 mm. **E**, tubeworm fossil from the early Jurassic Figueroa deposit, scale bar is 1 mm. **F**, abyssochrysoid gastropod from the Upper Cretaceous Kambia deposit (Troodos ophiolite), Cyprus, scale bar is 1 mm. **G**, portion of a transverse section through the wall of a mineralised

Alvinella tube preserved by pyrite and silica, scale bar is 2 mm. **H**, transverse section of a mineralised *Ridgeia piscesae* tube preserved by pyrite, scale bar is 250 µm. **I**, filamentous microbes preserved by pyrite within the tube wall of a mineralised *Alvinella* tube, scale bar is 10 µm. Preparation: F, secondary electron scanning electron microscopy (SEM) image of specimen extracted from rock matrix, G-I, backscatter SEM image of polished block preparations. Abbreviations: py, pyrite; si, silica.

2 Long-term preservation of hydrothermal vent deposits and fauna

Ancient hydrothermal vent deposits are distributed throughout the world's continents (Galley et al., 2007), but so far vent fossils (Fig. 2D-F) have been uncovered in only a subset of these (Fig. 3). For vent fossils to persist over geological time in a recognisable state, they must be incorporated into a deposit that escapes substantial metamorphic recrystallisation or destruction by subduction. Understanding the intricacies of vent deposit preservation provides important insights into the biases of the vent fossil record, as well as into where new fossil vent discoveries are most likely.

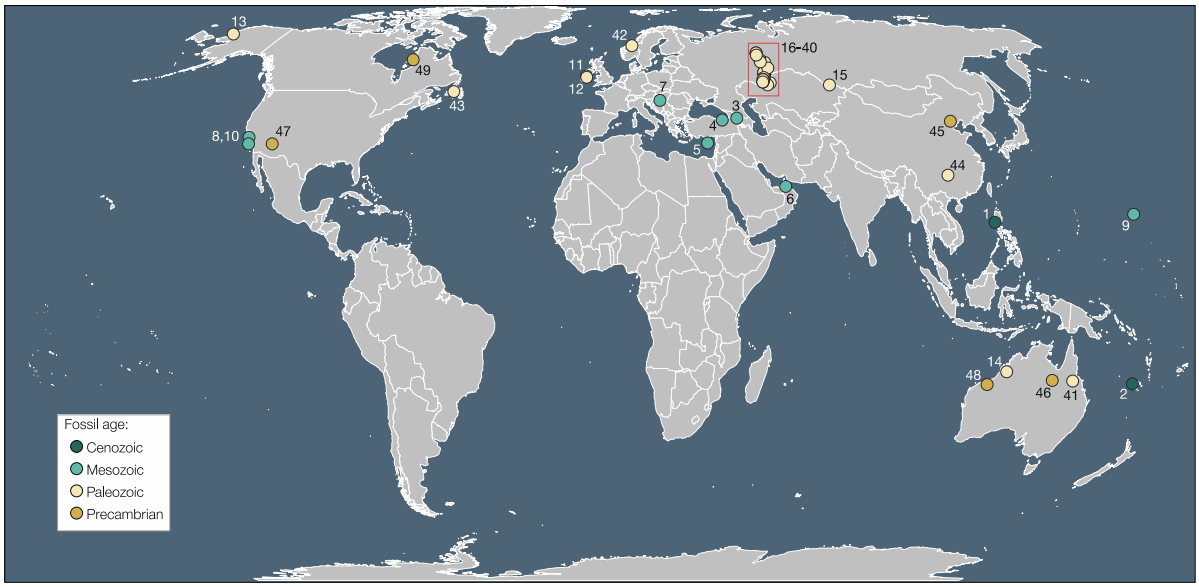

Figure 3. Ancient fossiliferous hydrothermal vent deposits categorised according to deposit age, box shows location of Fig. 4A. Labelled ancient vent deposits are as in Table 1: 1, Barlo, Philippines; 2, Azema, New Caledonia; 3, Madneuli, Georgia. 4, Lahanos, Killik, Çayeli, Kisilkaya, Turkey; 5, Kapedhes, Kinousa, Kambia, Memi, Sha, Peristerka, Cyprus; 6, Bayda, Oman; 7, Zengővárkony, Hungary; 8, Coast Range Ophiolite, USA; 9, OPD Core 129-801C-4R, W. Pacific; 10, Figueroa, USA; 11, Tynagh, Ireland; 12, Ballynoe, Ireland; 13, Red Dog, USA; 14, Canning Basin, Australia; 15, Nikolaevskoe, Kazakhstan; 16, Oktyabrskoe, Russia; 17, Barsuchiy Log, Russia; 18, Gaiskoe, Russia; 19, Alexandrinka, Russia; 20, Molodezhnoe, Russia; 21, Priorskoe, Kazakhstan; 22, Safyanovka, Russia; 23, Uzelga, Russia; 24, Talgan, Russia; 25, Babaryk, Russia; 26, XIX Parts'ezd, Russia; 27, Uchaly, Russia; 28, Sultanovka, Russia; 29, Sibay, Russia; 30, Buribay, Russia; 31, Yubileynoe, Russia; 32, Novo-Shemur, Russia; 33, Shemur, Russia;

34, Komsomol'skoe, Russia; 35, Blyava, Russia; 36, Dergamysh, Russia; 37, Krasnogvardeyskoe, Russia; 38, Ljeviha, Russia; 39, Valentorka, Russia; 40, Yaman Kasy, Russia; 41, Thalanga, Australia; 42, Løkken, Norway; 43, Tally Pond, Canada; 44, Niutitang Formation, China; 45, Gaobanhe, China; 46, Lady Loretta, Mt. Isa, McArthur River, Australia; 47, Jerome, USA; 48, Sulphur Springs, Australia; 49, Nuvvuagittuq belt, Canada.

Seafloor hydrothermal venting is one of the most important ore-forming processes on the Earth (Hannington et al., 2005). Ancient vent deposits contain mineral reserves that greatly exceed those calculated for SMS (Franklin et al., 2005), and thus have been mined for millennia (Laznicka, 2010). Ore deposits that formed in relation to ancient hydrothermal venting environments include both volcanic-associated massive sulfide (VMS) deposits and sedimentary-exhalative (SEDEX) deposits. There are recorded examples of fossil vent communities associated with both deposit types (Fig. 3; Table 1).

The geo-tectonic settings for SEDEX deposits are generally within rifted environments in continental settings, and only in rare cases is seafloor exhalation both demonstrated and preserved in such deposits (Leach et al., 2005). Many SEDEX deposits formed in restricted basins, often in highly reduced sedimentary settings where seafloor conditions were likely to be unfavourable for eukaryotic life (Leach et al., 2005). In contrast, as Franklin et al. (1981) pointed out, almost every tectonic setting with submarine volcanic rocks has the potential to host VMS deposits and hence there is a much broader range of ancient submarine settings where vent communities could develop in open seawater. There is a spectrum of VMS deposit types including some that have largely formed by sulfide replacement processes subsea-floor, whilst others have sulfides precipitated at or just below the sea floor and thus associated with direct seafloor venting over the life of the hydrothermal system (Doyle and Allen, 2003). Modern submarine oceanic settings where VMS deposits form include crustal spreading at mid ocean ridges, ocean hot spots and volcanic arcs (Hannington et al., 2005). Even so, not all modern systems have associated mega- or macro- vent faunal communities, particularly where unfavourable seafloor conditions are indicated or where mineral formation is largely by replacement in subseafloor sediments and volcanic rocks.

In the geological record, preservation of VMS deposits is largely restricted to deposits that formed in collisional environments during periods of extension and rifting (Franklin et al., 2005). Such environments, largely associated with supra-subduction settings, are the most likely seafloor sequences to be preserved in the ancient geological record. Mid-ocean ridge spreading zones, the most common site for modern hydrothermal vents, will become largely destroyed as seafloor crust is subducted as oceans close again by convergence. The preserved geological record of VMS deposits is therefore episodic, but includes important settings such as ophiolites as well as both oceanic and continental arc systems, that become preserved through accretion or obduction (Huston et al., 2010). Because preservation of VMS deposits is likely linked to orogenesis, many of the host sequences are as a result metamorphosed, often above greenschist facies, where primary seafloor features will be modified by dynamic recrystallisation. Systems where exceptional preservation is recorded are normally characterised by the preservation of textures within sulfides that record the submarine setting and show no evidence of overprinting (Herrington et al., 2005b). The exceptional case of Yaman Kasy, the best studied example in Ordovician-Silurian rocks of the Urals, yields key features to be expected in a well-preserved ancient vent system, including the sub-seafloor feeder stockwork system, massive sulfide mound, vent chimney/conduit debris, including chimney fragments and reworked interlayered sulfide, and oxide degraded mound sediments (Maslennikov, 1991; Herrington et al., 1998).

Devonian systems in the same tectonic domain of the southern Urals also show exceptional preservation resulting from the atypical evolution of the orogen (Brown et al., 2011). Comparative deposits in other tectonic units of the middle Urals are more highly deformed and to date have yielded no primary sulfide textures or fossils (Herrington et al., 2005b). Additionally, even in terranes where deposits have not experienced tectonic and metamorphic overprint, seafloor processes including halmyrolysis (the early diagenesis, modification, or decomposition of sediments on the sea floor) and diagenesis may have resulted in textural destruction of early features (Herrington et al., 2005c).

Fossiliferous deposits are recorded in a range of orogenic belts including the Urals (Paleozoic), Franciscan and Tethys (Mesozoic) and a number of more recent belts (Little et al., 1998). It follows that all VMS deposits that still preserve structures and textures indicative of seafloor processes have the potential to yield fossils. However, fossil preservation (taphonomy) plays a key role and the absence of fossils in a VMS deposit may not mean that vent biota was not living at that site while it was hydrothermally active. Overprinting geological processes will then serve to destroy any remaining evidence.

3 Preservation of biogenic structures within modern vent environments

Understanding how organisms are preserved at hydrothermal vents is central to interpretations of the fossil record of these environments, as well as providing remarkable insights into the discrepancies of fossilisation processes in general. The mineralisation of biogenic structures by minerals typical of vent settings constitutes a crucial first step in the formation of a vent fossil record. The precipitation of minerals from vent fluids that results in chimney formation also occurs on biological structures, and results in their mineralisation (the impregnation and/or replication of biological structures by typical vent minerals), a process which is aided by the general proximity of vent fauna to zones of vent fluid escape. Mineralisation of vent fauna can happen very rapidly, definitely within a year (Georgieva et al., 2015) and potentially within two weeks (Pradillon et al., 2009). Mineralised remains of vent fauna are readily found within modern vent sites and are essentially fossils, which can also be generated experimentally (Little, 2009).

3.1 Insights from the mineralisation of annelid dwelling tubes at high temperature vents

Fossilisation at hydrothermal vents is especially well documented for organic dwelling tubes produced by annelids in the families Alvinellidae and Siboglinidae (Fig. 2G-I) (Cook and Stakes, 1995; Maginn et al., 2002; Peng et al., 2008; Georgieva et al., 2015), but is not well understood for organisms which construct calcareous shells and tubes, such as molluscs and serpulid annelids. Organic annelid tubes are mineralised primarily by pyrite and silica within deep-sea hydrothermal vent environments. The

tubes of the vent siboglinid worm *Ridgeia piscesae*, which are originally comprised of a chitin-protein complex, are replaced primarily by pyrite following mineralisation (Fig. 2G) (Cook and Stakes, 1995). This mineralisation may be stimulated by microbes present within the tube wall (Peng et al., 2008, 2009). In the case of the multi-layered organic tubes produced by annelids of the genus *Alvinella*, mineralisation templates the surfaces of the organic tube layers (Zbinden et al., 2001; Maginn et al., 2002), resulting in a mineral tube that is also comprised of many concentric layers of iron sulfide minerals, predominantly pyrite (Fig. 2H) (Georgieva et al., 2015). Mineralisation of *Alvinella* tubes can result in variable preservation given the same starting structure (Georgieva et al., 2015), and can also be promoted by the presence of microbes within the tube wall (Maginn et al., 2002).

Studies of *Alvinella* tube fossilisation at hydrothermal vents have also revealed that preservation in this setting can be exquisitely fine-scale, with structures such as microbial cells, filaments, protein fibres and extracellular polymeric substances (EPS) also fossilised in remarkable detail by pyrite and silica (Fig. 2I) (Georgieva et al., 2015). The fine pyrite and/or silica templating that can occur at vents can also act to preserve details of fossil ornamentation, such as ridges on the surfaces of tube fossils, growth lines on gastropod and bivalve shells (Little et al., 2004a), or organic fibres that comprised the original walls of tube fossils (Georgieva et al., 2017).

3.2 Preservation within low temperature vent environments

At low temperature vent sites a proportion of the volume of iron oxyhydroxide precipitate is formed by benthic Fe-oxidising bacteria, principally belonging to the Zetaproteobacteria (Emerson et al., 2007; Davis et al., 2009; Chan et al., 2011, 2016a; McAllister et al., 2019). The best known of this group is *Mariprofundus ferrooxydans*, which has a bean-shaped cell that secretes very distinctive stalks, 0.6 to 2.2 μm wide and very often twisted, of organic-encased ferrihydrite, which precipitates on an organic template as a waste product from its metabolic activity. These stalks can then serve as a substrate for further iron oxyhydroxide precipitation, increasing the overall Fe/C ratio of the aging stalks (Chan et al., 2011). The stalks typically occur in parallel, a result of coordinated growth of cells

following a chemical gradient (Chan et al., 2016b). In addition to *M. ferrooxydans*, other Zetaproteobacteria are present at low temperature vent sites, forming different structures. These include unbranching cylindrical ferrihydrite-coated sheaths ca. 1 μm in diameter and hundreds of microns long (Fleming et al., 2013) and Y-shaped ferrihydrite-coated tubes ca. 2 to 4 μm in diameter and ca. 5 to 50 μm long (Emerson et al., 2007; Chan et al., 2016b). Zetaproteobacteria co-occur with other microorganisms at low-temperature vents to collectively form mat-like structures on the seafloor (e.g. Chan et al., 2016b; Johannessen et al., 2017; Vander Roost et al., 2017, 2018) that are partially organic and partially mineralogical. However, the main framework of these mats is formed by the Zetaproteobacteria. Whilst the micron-scale filaments formed by Zetaproteobacteria are not expected to have much in the way of preservation potential, silica precipitation often additionally occurs at low temperature vent sites (e.g. Rouxel et al., 2018), offering a taphonomic pathway for these highly delicate structures into the fossil record as jasper deposits.

3.3 Comparison of vent mineralisation with sites of exceptional preservation

Because of the mineralization of soft tissues (annelid organic tubes) and preservation of micron-scale morphological features and cells, fossilisation at hydrothermal vents can be compared with sites of exceptional preservation and terrestrial hydrothermal systems (Georgieva et al., 2015). At hot springs, silica can preserve microbes and plant tissues by direct replacement, templating or infilling (Jones and Renaut, 2003; Akahane et al., 2004), producing silica-comprised fossils that retain a level of detail similar to that observed within deep-sea vents. Exceptional preservation in soft sediment environments can occur through the growth of pyrite as framboids, pyritohedra, and euhedral crystals up to 20 μm in size that template or infill organic structures (Briggs et al., 1991, 1996). A variety of pyrite texture types also appear to be involved in the formation of fossils at deep-sea hydrothermal vents, notably colloform pyrite and framboids, but the pyrite that delineates hydrothermal vent fossils can also be exceptionally fine-grained (nanocrystalline) and may not necessarily be induced to form through the decomposition of organic matter (Georgieva et al., 2015).

4 The hydrothermal vent fossil record

Fossils were discovered within ancient hydrothermal vent deposits through mining activities long before the first observations of hydrothermal vents on the modern seafloor (Ivanov, 1947). Prior the late 1970s, the significance of fossils in VMS was not appreciated, but these have since been interpreted as vent fauna. The fossil record of hydrothermal vents is in general sparse. As detailed above, a fortuitous combination of circumstances are needed in order to preserve and locate fossils of hydrothermal vent fauna (Little et al., 1998). At the time of their last comprehensive review, hydrothermal vent macrofossils (Fig. 2D-F) were known from 19 deposits spanning the Ordovician-Silurian to the Eocene (Little et al., 1998). Additional deposits, as well as those containing only microbial fossils, were reviewed by Little et al. (2004b) and Campbell (2006), and extended the fossil record of vents into the Archean, 3.2 Ga. At this time, the vent fossil record was somewhat uneven, with only two fossiliferous deposits known from the Cenozoic, several more sites from the Mesozoic, a concentration of material from the Paleozoic primarily from the Ural Mountains region, and four Precambrian deposits containing microbial fossils only (Campbell, 2006).

From the material discussed within the above reviews, it is clear that life has existed at hydrothermal vents throughout much of Earth history, while metazoans are known to have exploited the high productivity of vents since at least the Silurian (Ivanov, 1959; Kuznetsov et al., 1993; Little et al., 1997, 1999c), or possibly the Ordovician (Buschmann and Maslennikov, 2006), based on uncertain dating of some of the oldest Urals fossil sites. As the vent fossil record exhibits strong bias towards organisms that form hard structures that are more resistant to decay (see section 2), many of the fossil sites are dominated by relatively few fossil types, usually including tubes considered to have been made by annelid worms.

When last reviewed, it was clear that vent environments appeared to have undergone major faunal transitions over evolutionary time (Little and Vrijenhoek, 2003; Vrijenhoek, 2013), largely dispelling a theory that they acted as evolutionary refuges in which relict taxa persisted unperturbed by major

world events such as mass extinctions (McLean, 1981; Newman, 1985). The Mesozoic appeared to mark a transition between vent faunas of the Paleozoic and Cenozoic, while molecular data largely demonstrated that many modern vent animals make their first appearances within chemosynthetic environments during the Cenozoic, which is also reflected by the fossil record of vesicomyid clams and bathymodiolin mussels (Kiel and Little, 2006; Vrijenhoek, 2013). The vent fossil record is especially poor during the Cenozoic, therefore much of what is known about the history of vent faunas from this time is inferred from the fossil record of cold seeps.

Since the reviews of Little et al. (1998) and Campbell (2006), fossils have been reported from 26 additional ancient hydrothermal deposits, spanning the Upper Cretaceous to the Eoarchean or possibly Hadean (Table 1; Fig. 3). The majority of these new occurrences are from the Paleozoic and are located within the Ural Mountains, revealing this to be particularly interesting and crucial region to the understanding of ancient vent communities. At the time of the above reviews, this region had already demonstrated considerable scientific significance having produced the most diverse ancient vent community known (Little et al., 1999c), and encompassing an especially high number of fossiliferous vent deposits (Fig. 3). The Ural Mountains region is given particular attention in Section 4.2.2. Evidence for the very early history of life within hydrothermal vents has also experienced major developments, as microbial fossils that very likely represent the earliest known organisms on our planet were recently discovered within an ancient marine vent environment (Dodd et al., 2017). Vent-associated deposits, such as sedimentary iron formations considered to have formed at the peripheries of high-temperature hydrothermal activity, have proved especially important to providing glimpses of early vent communities (Little et al., 2004b). In contrast, the fossil Mesozoic and Cenozoic hydrothermal vent fossil record has seen relatively few new discoveries. However, insights into ancient vent communities during this period may be gleaned from the fossil record of other chemosynthetic environments, as well as from molecular clock age estimates for recent vent fauna.

4.1 Precambrian

Five fossiliferous vent deposits exist from this time, spanning the Eoarchean-Hadean to the Mesoproterozoic, all of which feature filamentous microbial fossils and, in some instances, additional microbial structures (Table 1).

4.1.1 The earliest glimpses of life within hydrothermal precipitates: Nuvvuagittuq belt, Canada

The oldest known fossiliferous vent deposit occurs within the Nuvvuagittuq belt, Canada, and constitutes ferruginous sedimentary rocks 3.7-4.2 Ga in age, considered to have formed at a seafloor setting subjected to hydrothermal activity that produced vent-related precipitates (Dodd et al., 2017). These fossils occur as micrometre-scale hematite tubes and filaments, that resemble similar structures in jaspers associated with younger vent deposits (Grenne and Slack, 2003; Little et al., 2004b). In also representing the oldest direct evidence of life on Earth, the Nuvvuagittuq fossils highlight the importance of vent environments to the evolution of early life (Dodd et al., 2017), lending support to the theory that life itself may well have originated within a submarine hydrothermal setting (Martin et al., 2008; Deamer and Georgiou, 2015).

4.1.2 Paleoarchean to Mesoproterozoic vent fossils

The 3.2 Ga Sulphur Springs deposit records the first direct evidence of life within a high temperature vent environment, and contains filaments comprised of pyrite preserved within chert and coarse-grained quartz (Rasmussen, 2000). The biogenicity of these filaments has been questioned (Wacey et al., 2014), but considering that there is still a paucity of examples of nano-scale textures that may be generated from biogenic structures versus through abiotic processes, it remains possible that the Sulphur Springs filaments do indeed have a biogenic origin.

All other Precambrian instances of fossils at ancient vent environments date to the Mesoproterozoic, a period in Earth history when the first definitive eukaryotic fossils also emerge (Knoll et al., 2006; Butterfield, 2015). Filamentous microfossils 1.7 Ga in age observed within samples from the Jerome district of Arizona, USA, bear resemblance to those of Ordovician deposits such as Løkken, in both

morphology and preservation. They are also comprised of hematite and preserved within jasper considered to have formed within a deep-water hydrothermal setting (Slack et al., 2007; Little et al., 2021). The microfossil assemblage of the Lady Loretta, Mt. Isa and McArthur River deposits, Australia, is more diverse and includes both filaments and round cell morphologies (Oehler and Logan, 1977), preserved within black chert. The formation depth of these deposits is less well constrained, while biomarkers indicate the presence of sulfur-oxidising bacteria (Logan et al., 2001). A fairly diverse microfossil assemblage also occurs within the more recent, 1.4 Ga-old Gaobanhe Massive Sulfide, China, which features microfossils with filamentous, spherical, rod and coccus morphologies, and also contains the oldest known fossil vent chimneys (Li and Kusky, 2007).

4.2 Paleozoic

The major diversification of metazoans occurred during the early part of the Paleozoic, with these changes also reflected to an extent in the fossil record of hydrothermal vent environments. There are 34 fossiliferous vent deposits from this time period, the majority of which are Devonian age (Table 1), while recent reports have potentially identified the first Cambrian vent communities.

4.2.1 Cambrian-Ordovician vent fossils

Given that a diversity of metazoans appear well-established within hydrothermal vent environments by the early Silurian or late Ordovician (Little et al., 1999c; Buschmann and Maslennikov, 2006), it may be supposed that complex life may have colonised vents before this, rather than it taking 100 million years from the major diversification of animal life in the Cambrian to the eventual colonisation of vents by metazoans during the late Ordovician-early Silurian. At present, there are only two reports of metazoan fossils from hydrothermal vents that predate the early Silurian-late Ordovician: sponge spicules and double-walled tube fossils (approximately 1 mm in diameter) from a barite deposit of the Lower Cambrian Niutitang Formation, China (Yang et al., 2008), and smaller tube fossils (up to 80 μm in diameter) from metalliferous mudstones of the Middle Cambrian Tally Pond belt, Canada (Lode et al., 2016). Further investigations of material from Tally Pond have yielded a larger diversity of probable

metazoan structures, including a variety of tube fossils (15-125 μm in diameter), burrows (160 μm wide) and probable sponge spicules (Lode et al., 2020, *in prep.*). Together, these deposits provide intriguing indications that early metazoans from several metazoan phyla did venture into and potentially colonise vent sites. Although major Cambrian taxa such as trilobites are considered to have had the adaptations necessary to colonise hydrothermal vents (Fortey, 2000), their remains are yet to be found within ancient vent environments.

Ordovician vent fossils are represented by hematite filament networks that closely resemble structures created by iron-oxidising bacteria such as Zetaproteobacteria (McAllister et al., 2019). These occur in association with VMS deposits of the Løkken area of Norway (Grenne and Slack, 2003), and the Thalanga deposit, north-east Australia (Duhig et al., 1992a, 1992b; Davison et al., 2001).

4.2.2 The Paleozoic vents of the Ural Mountains

The fact that the Ural Mountains have yielded a large number of fossiliferous ancient vent sites (Fig. 4A; Table 1) is very likely due to their environment of formation and subsequent preservation history. Vent fossils are known from 25 Urals sites to date, with metazoan fossils reported from six new sites spanning the late Ordovician to the Middle Devonian. In addition, gossanites associated with a multitude of Urals vent deposits have yielded further microfossil finds, providing insights into additional aspects of these Paleozoic vent communities.

4.2.2.1 Geology of the Ural Mountains

The Uralide orogen (hereafter Urals) extends nearly 2500 km from the Aral Sea to Novaya Zemlya and records the Paleozoic collision of at least two intra-oceanic arcs with the margin of Laurussia and a final continent-continent collision with the Kazakh and Siberian plates (Brown et al., 2006, 2011). The paleo-Uralian ocean basin developed during Late Cambrian to Early Ordovician rifting. Early rift-stage rocks are found preserved in the Sakmara Allochthon (Fig. 4), which includes arc-related volcanics of Silurian or possibly Ordovician age that host the earliest fossiliferous VMS deposits found to date in

the Urals (Little et al., 1997; Herrington et al., 2002; Buschmann and Maslennikov, 2006). These allochthonous rocks have now been thrusted onto the continental margin rocks of Laurussia (Puchkov, 1997). The boundary between the continental margin of Laurussia and rocks of the Devonian Magnitogorsk oceanic arc system is marked by the Main Urals Fault (Fig. 4A), a complex suture containing a melange of serpentinites, high pressure rocks and thrusted sediments from the continental margin and oceanic rocks from the palaeo-Uralian ocean (Brown et al., 2006). East of the Main Uralian Fault lie the Magnitogorsk arc rocks of Mid-Devonian age, which are the main host to the fossiliferous VMS deposits in the southern Urals. The oldest, fore-arc rocks pass tectono-stratigraphically and geographically eastwards successively into arc, back-arc and inter-arc basin volcanic rocks that are host to a range of VMS deposits (Herrington et al., 2002, 2005a).

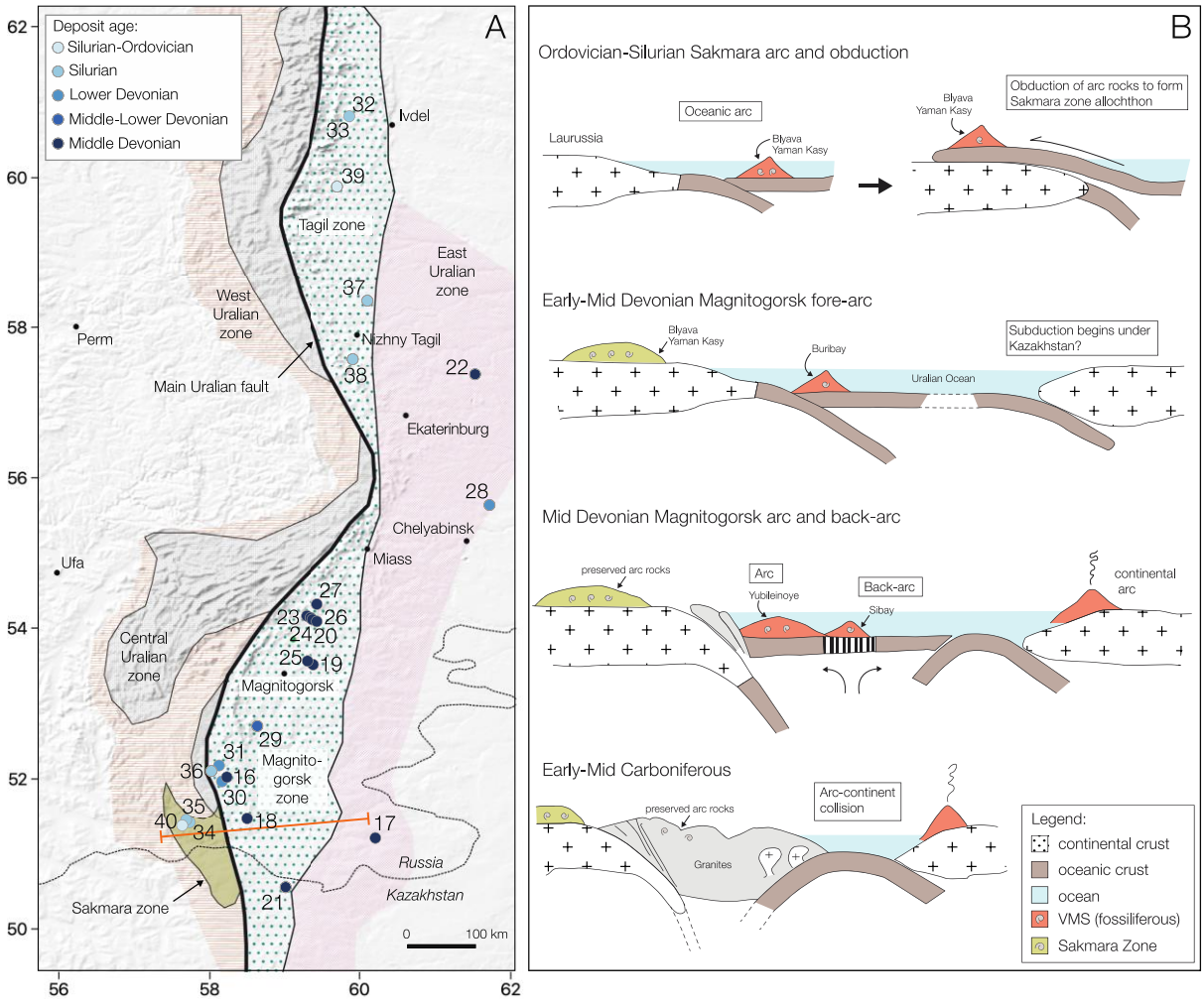

Figure 4. A, Fossiliferous vent deposits of the Ural Mountains region. Orange line indicates position of sections in B, labelled ancient vent deposits are as in Table 1: 16, Oktyabrskoe, Russia; 17, Barsuchiy Log, Russia; 18, Gaiskoe, Russia; 19, Alexandrinka, Russia;

20, Molodezhnoe, Russia; 21, Priorskoe, Kazakhstan; 22, Safyanovka, Russia; 23, Uzelga, Russia; 24, Talgan, Russia; 25, Babaryk, Russia; 26, XIX Parts'ezd, Russia; 27, Uchaly, Russia; 28, Sultanovka, Russia; 29, Sibay, Russia; 30, Buribay, Russia; 31, Yubileynoe, Russia; 32, Novo-Shemur, Russia; 33, Shemur, Russia; 34, Komsomol'skoe, Russia; 35, Blyava, Russia; 36, Dergamysh, Russia; 37, Krasnogvardeyskoe, Russia; 38, Ljeviha, Russia; 39, Valentorka, Russia; 40, Yaman Kasy, Russia. **B**, Schematic sectional cartoon showing time-slices illustrating tectonic evolution of the Urals. (i) Ordovician-Silurian, Sakmara arc developed marginal to the supercontinent of Laurussia. The VMS deposits of Yaman Kasy and Blyava developed in the Sakmara arc; (ii) Devonian – Sakmara zone (arc) obducted onto Laurussia margin, exceptional preservation of VMS deposits. Subduction skips to Magnitigorsk arc where fossiliferous VMS deposits including Oktyabrskoe, Yubileynoe, Sibay and Molodezhnoe developed; (iii) Late Devonian – Magnitogorsk arc collides with Laurussia margin as the margin becomes subducted, subduction skips east to East Uralian Zone and Turgai arc; (iv) Carboniferous – Final collision of Kazak continent assemblage and Laurussia margin to form the Urals, in southern Urals, Magnitogorsk arc rocks well preserved with little metamorphism.

VMS deposits of the Urals are classified into three-four types depending on the geological and geodynamic conditions of formation: Cyprus-Besshi, Urals, Baymak, and/or Kuroko (Zaykov et al., 1996; Prokin and Buslaev, 1999; Gusev et al., 2000; Herrington et al., 2002, 2005b; Glasby et al., 2007; Seravkin, 2010). These classifications can be broadly compared to the classifications of Franklin et al. (2005) where Cyprus is equivalent to Mafic, Besshi is related to Pelitic-mafic, Urals is considered to be Bimodal-mafic and Baymak represents Bimodal-felsic types. Cyprus-type deposits are typically hosted in tholeiitic basalts of Middle Devonian age formed in the Dombarovsk and West Mugodjar back arc basins that developed behind the Magnitogorsk arc (Fig. 4B). The Buribay deposit is hosted in boninitic basalt and gabbro of the lowermost part of Baymak-Buribay Formation, in the fore-arc position of the Magnitogorsk arc (Herrington et al., 2005b). These deposits are all dominated by Cu and consist mainly of chalcopyrite and pyrite with minor sphalerite. The Ural-type deposits are hosted in bimodal basalt-rhyolite sequences and occur in the basal parts of Tagil arc (see Fig. 4A), West and East Magnitogorsk island-arc and Sibay back-arc basins. An evaluation of the settings with which vent fossils in the Urals are associated revealed that ancient vent fauna mainly occur in massive sulfide mounds formed in jasper-associated basalt and basalt-rhyolite formations, but are less common in serpentinite formations. The probability of finding fossils appeared to correlate with the relative abundance of basalt versus felsic volcanic rocks that underlie the deposits (Maslennikov et al., 2017).

4.2.2.2 Urals vent fossils

Since the reviews of Little et al. (1998) and Campbell (2006), metazoan fossils have been additionally reported from the Blyava, Dergamysh, Molodezhnoe, Priorskoe, Sultanovka and Valentorka VMS deposits (Maslennikov et al., 2016, 2017) (Fig. 5), microbial fossils have been documented in detail from Yaman Kasy (Georgieva et al., 2018), and tube structures that could represent either small metazoans or large microbes have been discovered in hydrothermal sedimentary rocks associated with the Alexandrinka, Babaryk, Blyava, Molodezhnoe, Shemur, Novo-Shemur, Priorskoe, Sibay, Talgan, Uchaly, XIX Parts'ezd and Yaman Kasy VMS deposits (Ayupova et al., 2017) (Fig. 6).

The late Ordovician-early Silurian Yaman Kasy deposit hosts the oldest vent community that includes definitive metazoans, which is also the most diverse ancient vent community known. This deposit contains two fossil types of probable annelid tubeworms, two lingulid brachiopods, an ambonychiid bivalve, a monoplacophoran, an indeterminate vetigastropod, and an indeterminate double-shelled fossil (Little et al., 1999c; Buschmann and Maslennikov, 2006). The worm tubes contained within this deposit (the fossil species *Yamankasia rifeia* and *Eoalvinellodes annulatus*) were initially likened to those produced by modern vent lineages, notably vestimentiferans and Alvinellidae respectively (Little et al., 1997, 1999c). *Y. rifeia* tubes (Fig. 5A) have size ranges of 3-39 mm in diameter (Little et al., 1999c), and hence are comparable in size to the modern siboglinid species *Riftia pachyptila*, or giant tubeworm. *E. annulatus* tubes are smaller, typically 0.1-3.5 mm in diameter, and occur close to vent chimney structures and have therefore been compared to present-day tubicolous alvinellid species. However, ornamental characters present on annelid tubes can often exhibit convergence (Kiel and Dando, 2009), while a Silurian or Ordovician fossil age for vestimentiferans and alvinellids appears to be inconsistent with origination dates indicated for these lineages by molecular clocks (Vrijenhoek, 2013). A recent re-examination of the Yaman Kasy tube fossils suggested that they are unlikely to have been built by annelid lineages that inhabit present-day vent environments (Georgieva et al., 2017). The Yaman Kasy brachiopods and monoplacophorans belong to extinct Paleozoic higher taxa. The microbial fossils recently documented from this deposit are associated with the surfaces of worm

tubes (Little et al., 1997; Maslennikov, 1999; Georgieva et al., 2018), indicating that symbiotic interactions between animals and microbes were similar to those that occur within present-day vent environments, where annelid tubes provide important habitat for diverse microbial communities (Lopez-Garcia et al., 2002; Campbell et al., 2003; Duperron et al., 2009). The Yaman Kasy microbial fossils also demonstrate that sub-micron fossil textures can be retained over hundreds of millions of years in VMS deposits not subjected to significant metamorphism, confirmed by preservation of delicate sulfide textures in associated vent chimney material (Herrington et al., 1998).

Other Urals vent deposits dating to the Silurian (Blyava, Dergamysh, Krasnogvardeyskoe, Komsomol'skoe, Ljeviha, Novo-Shemur, Shemur, and Valentorka) contain mainly worm tubes (Fig. 5B-D). These tubes are typically 1-3 mm in diameter, with some tube-like structures from Dergamysh being potentially larger (Fig. 5E), while additional textures found in material from Dergamysh represent collomorphic textures consistent with microbialites (Fig. 5F). The majority of tube fossils from the Blyava, Valentorka and Dergamysh deposits are comparable to the size range of *Eoalvinellodes annulatus*, however their mode of preservation renders it difficult to observe tube wall characteristics, and hence to compare directly to better-preserved material from Yaman Kasy, or to present-day tubicolous animals. The Ljeviha deposit is also reported to contain brachiopods (Ivanov, 1959), but unfortunately this material is no longer available for study (Little et al., 1998).

The majority of fossiliferous Urals vent deposits are Middle Devonian in age, with only Buribay, Yubileynoe, and Sibay (Fig. 5G-I) dating to the Lower or Lower-Middle Devonian (Table 1). The Sibay deposit has yielded the most diverse ancient vent community from the Devonian, containing metazoan fossils of two types of worm tubes (*Tevidestus serriformis* (Fig. 5I) and indeterminate ?annelid worm tubes), the modiomorphid bivalve species *Sibaya ivanovi*, as well as indeterminate bivalves or brachiopods. The tubes of *T. serriformis* have also been likened to those made by vestimentiferans, particularly the modern species *Tevnia jerichonana* in virtue of the presence of closely-spaced collars or flanges present on the outer walls of both tube types. Recent reanalysis of *T. serriformis* tubes

revealed that they were also preserved with an astonishingly fine mesh of pyritised fibres present on the outer tube wall (Fig. 5I), which cross at near right angles (Georgieva et al., 2017). A similar fibre arrangement occurs on the tubes of modern chaetopterid worms (Annelida: Chaetopteridae) (Bhaud, 1998; Shah et al., 2015). Chaetopterids can also be common in modern vent environments (Morineaux et al., 2010; Okumura et al., 2016) and are deemed to have ancient origins, having diverged from other annelids during early stages of the diversification of this phylum (Weigert et al., 2014; Weigert and Bleidorn, 2016). It is therefore possible that *T. serriformis* fossils from Sibay may represent the earliest known fossils of chaetopterids, but the additional presence of vestimentiferan-like characters render them difficult to place definitively (Georgieva et al., 2017).

The fossil tubes present within material from Yubileynoe are remarkable for the dense clusters they form in very close proximity to vent chimneys (Fig. 5H). These tubes are within the size range of the Yaman Kasy species *Eoalvinellodes annulatus*, but the outer tube wall details have not been observed and it is therefore not known if the Yubileynoe tubes are closely related. Worm tubes from Buribay are small, typically less than 1 mm in diameter (Fig. 5G), and are also difficult to identify in virtue of few distinguishing characters.

Nearly all Middle Devonian ancient vent deposits from the Urals contain worm tubes (Fig. 5J-L) (with the exception of Babaryk and XIX Parts'ezd), while brachiopods have additionally been observed at the Oktyabrskoe site (Table 1). Therefore, metazoans appear to have been prevalent within Devonian vent sites, but their apparently low diversity is surprising, given the greater numbers of taxa uncovered within the Yaman Kasy and Sibay deposits. This could be a result of biases in fossilisation as well as fossil discovery, as the findings at Middle Devonian Urals sites largely represent opportunistic finds rather than systematic palaeontological field surveys. Given the above in addition to the occurrence of probable metazoan fossils at such a great number of Middle Devonian Urals ancient vent sites, it appears that life at these vent sites was well-established, with most vent sites inhabited by abundant tube-dwelling metazoans that were likely among the dominant taxa at these sites.

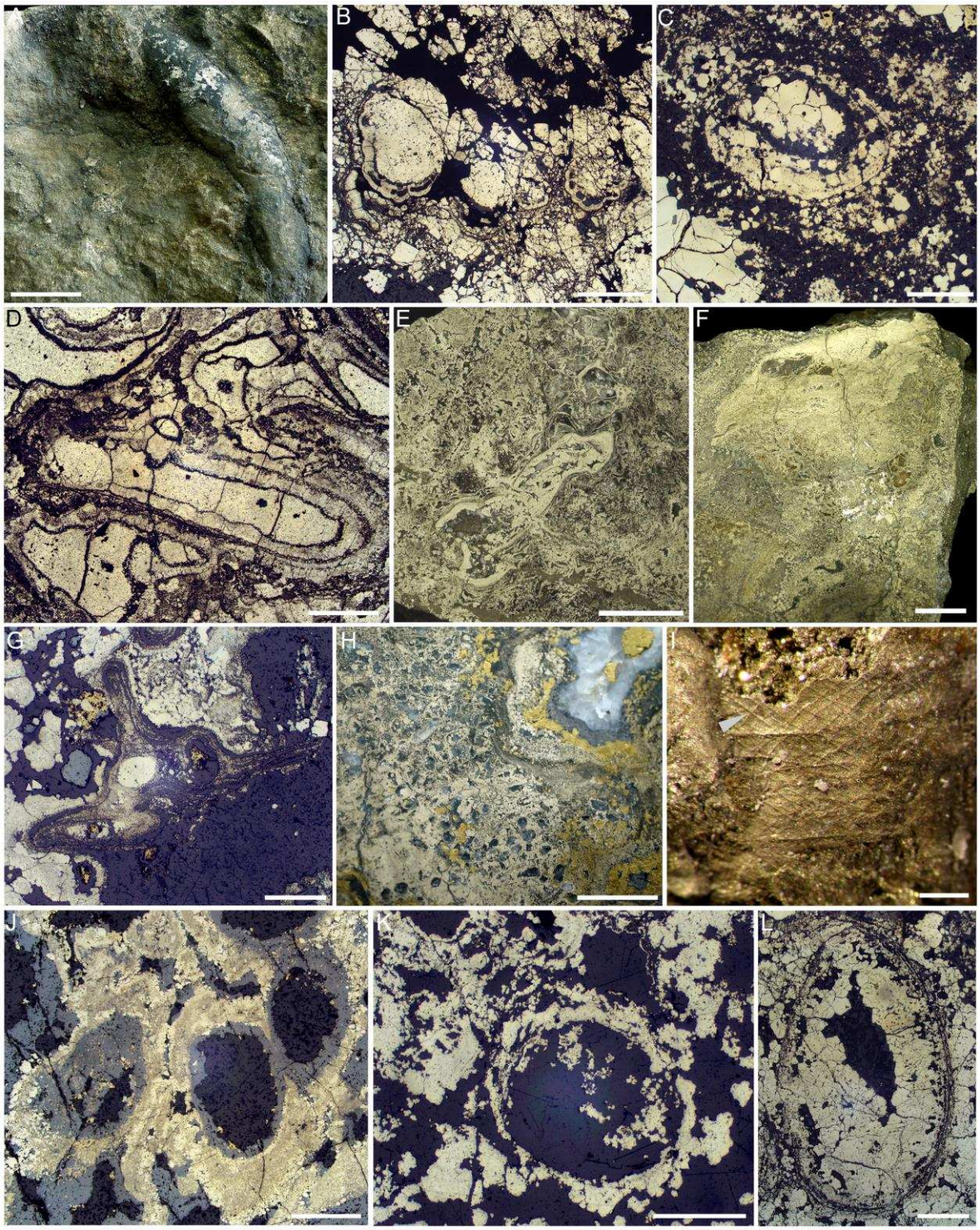

Figure 5. Fossils from Urals ancient vent deposits. **A**, the large tube of *Yamankasia rifeia*, Yaman Kasy, scale bar is 30 mm. **B**, tube fossils in transverse section, Blyava, scale bar is 1 mm. **C**, tube fossil in transverse section, Valentorka, scale bar is 1 mm. **D**, small tube fossils, Dergamysh, scale bar is 1 mm. **E**, large tube-like structure, Dergamysh, scale bar is 20 mm. **F**, microbialitic texture, Dergamysh, scale bar is 20 mm. **G**, tube fossils, Buribay, scale bar is 1 mm. **H**, tube fossils adjacent to vent fluid conduit, scale bar is 10 mm. **I**, detail of the outer wall of a *Tevidestus serriformis* tube, Sibay, arrow shows preserved tube wall fibres. Scale bar is 1 mm.

586 **J**, tube fossils in transverse section, Molodezhnoe, scale bar is 1 mm. **K**, tube fossil in transverse section, Priorskoe, scale bar is 1
587 mm. **L**, tube fossil in transverse section, Sultanovka, scale bar is 1 mm. Preparation: B-D, G, J-L, reflected light images of polished
588 block preparations. E-F, H, photographs of polished slabs.
589
590

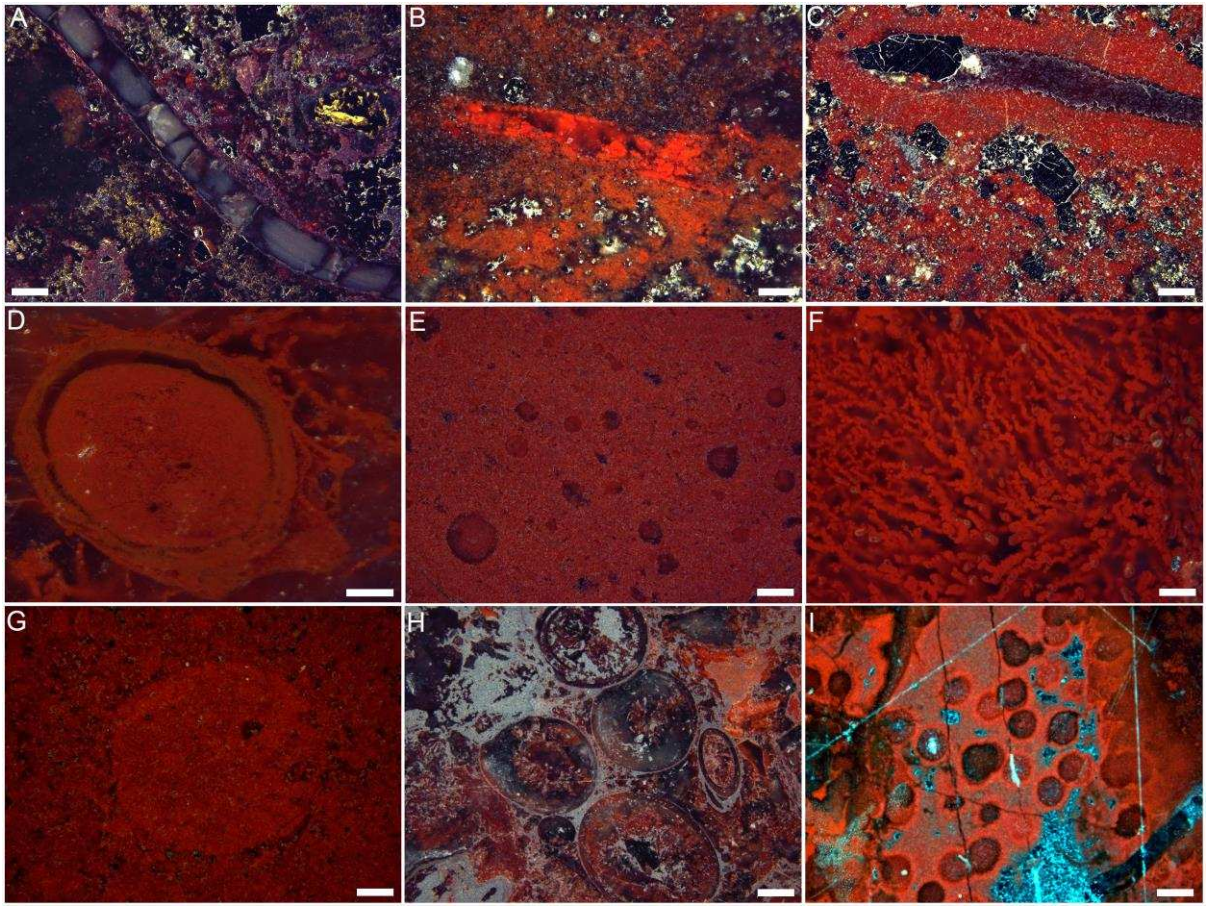

591
592 **Figure 6**. Fossils from gossanites associated with Urals Ordovician-Silurian (A-C) and Devonian (D-I) ancient vent deposits. **A**,
593 tube/filament fossil, Yaman Kasy, scale bar is 60 µm. **B**, walled tube-like fossil from Shemur, scale bar is 60 µm. **C**, Tubular structure
594 from Novo-Shemur with a thick Fe-oxide wall, scale bar is 120 µm. **D**, transverse section of tube fossil from Yubileynoe, scale bar is
595 120 µm. **E**, tube fossils from Sibay, scale bar is 30 µm. **F**, Fe-oxide filament network from the Sibay deposit, scale bar is 60 µm. **G**,
596 transverse section of a tube fossil from Uchaly, scale bar is 60 µm. **H**, cluster of tube fossils in transverse section from Molodezhnoye,
597 scale bar is 120 µm. **I**, cluster of spherical structures from Alexandrinka, scale bar is 120 µm. Preparation: all, transmitted light images
598 of thin section preparations.
599
600

601 The majority of fossils discovered within gossanites from the Urals are small, up to 550 µm in diameter
602 in the case of tube fossils (Ayupova et al., 2017) (Fig. 6A-E, G-I). A subset of tube fossils exhibit

possible internal ornamentation (Fig. 6A), distinctive walls (Fig. 6B-D, H), and also appear to be directly attached to others (Fig. 6H). These tube fossils are associated with a range of additional textures such as filaments that resemble those of Fe-oxidising bacteria (Fig. 6F), and clusters of spherical structures up to 120 µm in diameter that interlock with others (Fig. 6I). Smaller spheres ~15 µm in diameter were also found to inside tubes (Ayupova et al., 2017), and clusters of the above may also fill tube cavities, and are considered to also have microbial origins. Between tube fossils, shorter radial filaments 10 µm in diameter have been observed, that have been likened to fungal hyphae (Ayupova et al., 2017).

4.2.3 Devonian and Carboniferous vent fossils beyond the Urals

Devonian and Carboniferous ancient vent sites beyond the Urals are again mostly dominated by macro- to megafaunal-sized worm tube fossils. Tubes from the Carboniferous Ballynoe and Tynagh deposits, Ireland, are 2.5 mm and up to 0.8 mm in diameter, respectively (Boyce et al., 2003). While somewhat different in size, they both exhibit distinct tube wall ornamentation of closely-spaced annulations, which led Boyce et al. (2003) to conclude that they are likely related. Tube fossils from the Carboniferous Red Dog deposit are larger (3-9 mm in diameter), are not preserved with any ornamentation, and are associated with pellets 1-2 mm in diameter that could represent fecal matter, algal debris, or microbial clumps (Moore et al., 1986). No metazoan faunas have been discovered within with the Canning Basin reefs of Western Australia, which comprise extensive stromatolites that in association with inorganic deposits form mounds hundreds of metres long and tens of metres thick, that are preserved within sedimentary exhalative deposits formed as a result of the ejection of relatively cool fluids from the seafloor (Playford and Wallace, 2001). The stromatolites are comprised of carbonate possibly formed through bacterial oxidation of organic matter, and are interpreted to have formed within deep inter-reef basins, bounded by anoxic muds.

4.3 Mesozoic

A number of vent fossil sites are recorded from Mesozoic VMS deposits, mostly from the Upper Cretaceous Tethyan palaeo-oceanic sequences (Fig. 7). These include important, taxonomically diverse sites in the Troodos ophiolite in Cyprus (Little et al., 1999a) as well as sites of tubeworm fossils in Georgia, Turkey and Oman. A single Jurassic occurrence containing metazoan fossils is recorded in the Franciscan complex of western USA (Little et al., 1999b, 2004a).

4.3.1 Jurassic to Lower Cretaceous vent faunas

All three known Jurassic-age ancient vent localities contain microbial filaments preserved within jasper, while only the Figueroa site hosts metazoan fossils (Table 1). The Figueroa site is the oldest known ancient vent locality from the Mesozoic, and hosts a specimen-rich but low diversity assemblage of worm tubes 0.3 to 6.8 mm in diameter (Fig. 2E), rhynchonellid brachiopods (*Anarhynchia* cf. *gabbi*), and trochoidean gastropods (*Francisciconcha maslennikovi*) (Little et al., 1999b, 2004a). Worm tubes preserved within the Figueroa deposit have also been likened to those of vestimentiferans (Little et al., 1999b, 2004a). In this instance, recent re-examination has affirmed that vestimentiferans are the most likely candidates to have constructed the Figueroa tubes (Georgieva et al., 2017). This would suggest a 190 Ma (million year) history of vestimentiferans in the Pacific Ocean (Little et al., 2004a), however this still precedes the oldest molecular age estimates for this lineage by approximately 70 Ma (Vrijenhoek, 2013). The Figueroa rhynchonellid brachiopod species belongs to the now extinct Dimerellidae family, while *Francisciconcha maslennikovi* is the first known fossil trochoidean from chemosynthetic environments. Trochoidea also occur within present-day vent communities, therefore the Figueroa fossil vent site appears to illustrate a transition between Paleozoic and Mesozoic vent communities.

Brachiopods are also abundant within the iron ore deposit of Zengővárkony, Hungary, which is deemed to have formed in association with hydrothermal activity in a continental rift setting (Bujtor and Vörös, 2020). At least eight brachiopod species are reported from this site (Table 1), with the sizes of two of these (*Lacunosella hoheneggeri* and *Nucleata veronica*) being on average 30 to 70%

larger than specimens from their respective type localities (Bujtor, 2006, 2007). This size increase has been inferred to result from the above brachiopod species having benefitted from hydrothermal productivity. As certain modern vent animals (e.g. the giant tubeworm *Riftia pachyptila*, the giant clam *Calyptogena magnifica*) achieve large body sizes through efficiently harnessing the high productivity at hydrothermal vents, large body sizes of fossil vent and seep animals has been suggested as a proxy for a potential chemosymbiotic lifestyle (Sandy, 1995).

4.3.2 The Upper Cretaceous Tethyan realm

Fossiliferous deposits, so far discovered, in the Neotethys realm (which separated Gondwana from the Cimmerian microcontinents during the Mesozoic) formed in two distinct tectonic settings (Fig. 7). The Troodos and Samail ophiolites are both developed in comparable settings at the supra-subduction fore-arc of the south Neotethys (Fig. 7). In the case of Samail, the 96 Ma ophiolite-hosted VMS deposit formed in a fore-arc setting and then was rapidly obducted onto the Arabian plate within a few million years (ca. 92 Ma) where it is now preserved and the deposits exposed (Searle et al., 2015). The deposits in Troodos, Cyprus, likely formed in an analogous geo-tectonic position to Samail, Oman, around 94 Ma (Chen et al., 2020; Morag et al., 2020), with the island of Cyprus still sitting over the subducted continental margin of the African plate with uplift and exposure of the ophiolite sequence only occurring in Miocene times (Robertson et al., 2012).

The Madneuli and Turkish VMS localities developed in supra-subduction arc settings along the northern margin of the Neotethys. Here, arc volcanics developed on continental crust in a string of VMS deposits that includes the fossil localities of Lahanos, Killik, Çayeli and Kisilkaya in Turkey and Madneuli in Georgia (Fig. 7). Deposits are all believed to be Upper Cretaceous in age, ±94-88 Ma (Little et al., 2007; Revan et al., 2017), being preserved when the northern branch of the Neotethys closed at the end of the Cretaceous (Robertson et al., 2012).

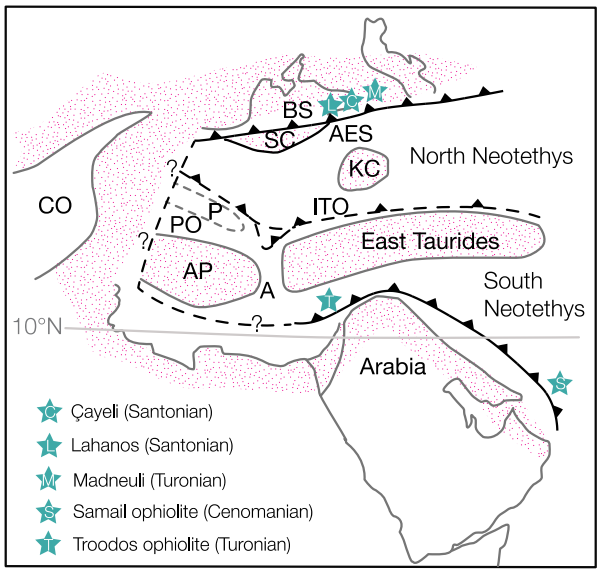

682

683 **Figure 7**. Geo-tectonic setting of the Tethyan fossiliferous VMS deposits Modified from Little et al., (2007). Killik and Kizilkaya are
684 both located near Lahanos. A, Antalya; AES, Ankara-Erzincan suture; AP, Apulia; BS, Black Sea; CO, Carpathian ocean; KC,
685 Kirsehir continent; ITO, Inner Tauride ocean; P, Pelagonian microcontinent; PO, Pindos ocean; SC, Sakarya continent.

686

687 Only worm tube fossils have been found so far from the Bayda, Madneuli and Turkish sites, while
688 localities from Cyprus have yielded more diverse assemblages that include at least three types of
689 worm tubes (Georgieva et al., 2017), eight new species of abyssochrysoid gastropods (Fig. 2F)
690 (Andrzej Kaim, 2020, *pers. comm.*), as well as microbial filaments in jasper (Little et al., 1999a). One
691 of the worm tube types, described as 'wrinkled' in Georgieva et al. (2017), also shows close similarities
692 with the tubes of vestimentiferans, while the other two tube types demonstrate characteristics that are
693 consistent with both vestimentiferan and serpulid annelids. The abyssochrysoid gastropods comprise
694 the families Provannidae and Abyssochrysidae, along with the extinct families Hokkaidoconchidae and
695 Paskentanidae (Sasaki et al., 2010; Kaim et al., 2014), and the Cyprus specimens represent the first
696 record of this lineage within a vent deposit. Worm tubes from Bayda are 1-5 mm in diameter, and can
697 exhibit annulations that are very closely-spaced in some specimens (Haymon and Koski, 1985). Tubes
698 from the Turkish sites and Madneuli do not have discernible ornamentation, and are larger than those
699 from Bayda having diameters of up to 25 mm and 6.5 to 13.1 mm respectively (Little et al., 2007;
700 Revan et al., 2010).

701

4.4 Cenozoic

The two known Cenozoic examples of fossiliferous VMS deposits are both located in the western Pacific in preserved dominantly mafic volcanic packages, and both contain only worm tube fossils. The Azema fossil locality in New Caledonia comprises a small copper-barite bearing VMS deposit developed in Senonian to Paleocene basalts that are part of the Poya terrane. The Poya terrane likely represents rocks scraped off the ocean floor of the western Pacific onto the basement terranes of New Caledonia as the lower plate of the Loyalty Basin was subducted westwards under the island (Ulrich et al., 2010). The Poya terrane has since been overthrust by older Eocene peridotite 'massifs' that have later become deeply weathered to form the extensive nickeliferous laterites of the island. The tectonic position of the deposit and its host sequence at time of formation is unclear, although the volcanics show mid-ocean ridge, back-arc basin and ocean island affinities (Ulrich et al., 2010). The Azema worm tubes are small with diameters of 0.2-0.3 mm, with some specimens also exhibiting transverse annulations (Oudin et al., 1985).

The Barlo VMS copper-zinc deposit, is hosted in the middle Eocene (ca. 44 Ma) Zambales ophiolite sequence in western Luzon, Philippines. The mine sequence is dominated by basaltic lavas and contains units of boninitic affinity, indicative of a supra-subduction zone fore-arc setting (Perez et al., 2018). These volcanic rocks have similar chemistries to units hosting the VMS occurrences in the Oman and Troodos ophiolites, consistent with them all sharing an analogous geo-tectonic setting and thus may be classified as a Cyprus-type deposit *ss*. These tubes are approximately 5 mm in diameter and have thick walls (150 µm) (Boirat and Fouquet, 1986), but have been observed mainly in section therefore details of any wall ornamentation and thus their identity are unknown.

5 Insights from phylogenetics

Molecular tools are widely employed to assess the evolutionary history of vent fauna, and are especially useful in the case of taxa that do not normally leave a fossil record (Kumar, 2005). Molecular clock analyses, which comprise the application of an approximately uniform evolutionary rate over

time to infer the age of lineages, can however suffer from limitations such as assumptions of the rate and stability of genetic evolutionary change. They are best applied when they can be calibrated with direct fossil evidence, but even then are not altogether reliable (Louca and Pennell, 2020). Nevertheless, patterns among molecular clock estimates for different taxa along with consistencies with the fossil record can provide further insights into the evolutionary history of vent environments.

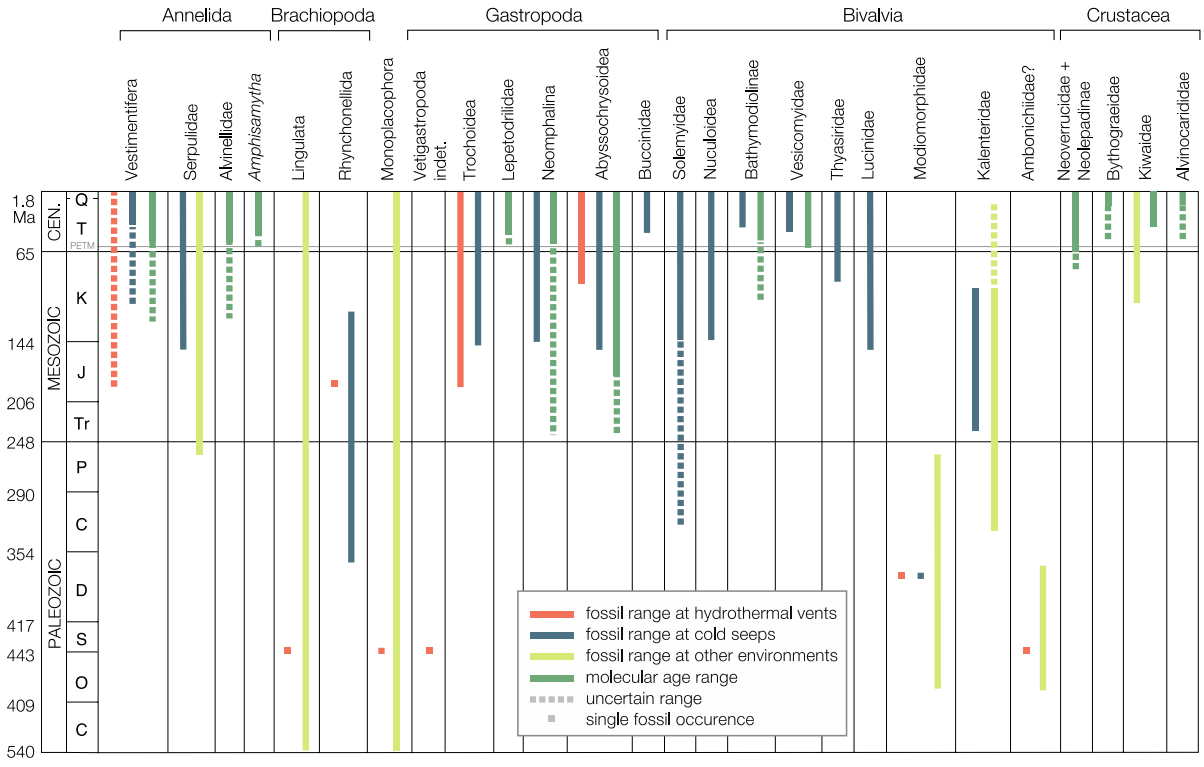

Figure 8. Fossil and molecular origination range estimates for taxa encountered within vent environments. Figure adapted from Little and Vrijenhoek (2003) and Georgieva (2016) with updated data (Vrijenhoek, 2013; Lorion et al., 2013; Vinn et al., 2013; Herrera et al., 2015; Georgieva et al., 2017; Sanfilippo et al., 2017; Sun et al., 2017, 2018; Roterman et al., 2018; Li et al., 2019; Breusing et al., 2020). PETM, Paleocene-Eocene Thermal Maximum.

When last reviewed by Vrijenhoek (2013), molecular age estimates for taxa that dominate modern vent sites suggested largely Cenozoic radiations, occurring especially after the Paleocene-Eocene thermal maximum (PETM), a period during which anoxic/dysoxic conditions are considered to have prevailed in much of the world's deep ocean basins (Kennett and Stott, 1991). Cenozoic radiations for vent taxa are still apparent when more recent studies on symbiotic deep-sea mussels, kiwaid anomurans, and alvinocaridid shrimp are taken into consideration (Fig. 8) (Lorion et al., 2013;

747 Roterman et al., 2018; Sun et al., 2018). However, other lineages such as abyssochrysoid gastropods
748 appear to have originated and diversified during the Mesozoic. Vestimentiferans, alvinellids, as well as
749 some vent limpets and barnacles also seem to have their origins within the Mesozoic, which in the
750 case of Neomphalina is confirmed by their fossil record at seeps. None of the lineages occupying
751 present-day vents are considered to have originated in the Paleozoic. Molecular age estimates
752 therefore largely confirm the pattern indicated by the fossil record of vent environments having
753 undergone a major faunal transition following the Paleozoic, and that modern vent communities are
754 occupied by lineages which originated either during the Mesozoic or Cenozoic. Molecular age
755 estimates can however demonstrate large ranges of uncertainty, for example spanning 75 Ma for the
756 vestimentiferans (Li et al., 2019), and thus it may be unsubstantiated to attribute Cenozoic radiations
757 to a discrete event such as the PETM. For some vent lineages, molecular age estimates also suggest
758 that origination dates greatly preceded diversification events, for example by up to 80 Ma in the case
759 of alvinellid annelids (Vrijenhoek, 2013), which in combination with the paucity of the fossil record
760 makes it difficult to speculate on what may have happened in between.
761

762 ## 6 Perspectives and future directions

763 The fossil record of ancient vent environments, in combination with molecular data from modern vent
764 animals, demonstrates that hydrothermal vents have been important habitats for life, possibly since its
765 origination, as well as for complex multi-cellular life soon after its diversification during the Cambrian.
766 Whether life itself began at hydrothermal vents remains a debated question, that since the discoveries
767 of the Nuvvuagittuq fossils by Dodd et al. (2017) is also weaved into the discussion of what constitutes
768 the oldest fossil evidence of life on our planet (Benton and Harper, 2020). Contenders for the oldest
769 fossil in the world come from a range of palaeo-environments (Lepot, 2020), while molecular evidence
770 suggests that the last universal common ancestor (LUCA) of all cells was likely thermophilic and lived
771 in an environment rich in sulfur (Weiss et al., 2018). Biosignatures have been reported from a range
772 of Paleo- to Mesoarchean environments that experienced hydrothermal activity, demonstrating that
773 life was well-adapted to such settings from very early on in its history (Sugitani et al., 2015).

Hydrothermal vents likely constituted important habitats for early life on Earth, with fossil insights from the Precambrian indicating that they were readily exploited by microbes. The microbial communities of vents, within both vent-peripheral and high-temperature vent settings, were therefore likely well-established billions of years before the onset of animal life.

The Cambrian Tally Pond fossil faunas (Lode et al., 2020, *in prep.*) hint that metazoans probably did begin to move into vent environments during the Cambrian, with metalliferous mudstones forming on the peripheries of vent fields potentially providing underexploited food sources in the form of microbial mats, as well as ideal conditions for early animals to acclimatise to the harsher conditions that prevail in closer proximity to chimneys. The Urals faunas remain the best-preserved examples of Paleozoic vent communities, in which both vent environments and faunas were fossilised in remarkable detail, and demonstrate that by the late Ordovician or early Silurian, certain animals had adapted to vent conditions so effectively as to be able to colonise the walls of active vent chimneys, as observed for the fossil tubeworm *Eoalvinellodes annulatus* (Little et al., 1999c). It therefore appears that Paleozoic vent faunas were exploiting vent niches effectively, rather than opportunistically straying into vent environments. These ancient vent animals may have also developed symbioses with microbes capable of chemosynthesis, due to their large sizes and high abundances. However, this is very difficult to prove definitively. The extraordinary fine-scale preservation at Yaman Kasy has revealed that microbes were intimately associated with the surfaces of vent animals (Georgieva et al., 2018), thus potentially paving the way for more highly-integrated relationships. The sheer abundance of both microbial and metazoan life, as indicated by the multitude of fossils from the Urals, reveals the critical importance of vents as habitats for Paleozoic marine life. The Urals represent an oceanic arc system analogous to the western Pacific today, in which faunal distributions are spatially delimited by oceanographic barriers (Mitarai et al., 2016; Breusing et al., 2020). It is possible that similar factors also controlled the distributions of Urals ancient vent faunas, whereby highly-connected vent fields shared tubeworm species, while more isolated vents provided suitable conditions for taxa not already adapted to vents to move into these environments.

The number of known fossiliferous ancient vent sites tails off rapidly following the Carboniferous, which brings about the question of whether this indicates an absence of evidence of vent faunas, or evidence of absence. The preservation of VMS deposits is intimately tied to cycles of continental rearrangement, of which there have been three major peaks during Earth history: 2.74-2.68 Ga (Archean), 1.9-1.76 Ga (Proterozoic) and 520-300 Ma (Paleozoic) (Huston et al., 2010, 2015). In simple terms based on the volume of metal sulfides so-far found in VMS deposits, the Mesozoic is significantly less productive for VMS deposits than the Paleozoic, with the Cenozoic being particularly less productive. This is likely as a result of reduced tectonic activity in the later Eras leading to fewer deposits than the more dynamic preceding periods of Earth history. Given how few ancient vent deposits are sufficiently well-preserved to yield fossils, it is reasonable to expect fewer vent fossil sites during the Mesozoic and Cenozoic.

While some animal types, notably brachiopods, appear to have continued to colonise vents from the Paleozoic and into the Mesozoic, it is increasingly clear that modern vent lineages began to move into vent environments during the Mesozoic or Cenozoic. This is a pattern which is apparent from fossil evidence of both hydrothermal vent and cold seep environments, as well as that of molecular clocks (Fig. 8). The end-Permian mass extinction likely had profound impacts on life in the deep ocean (Brennecka et al., 2011; Chen and Benton, 2012) from which it took several million years to recover (Chen and Benton, 2012), and it is plausible that this may have instigated a shift in vent faunas. However, a paucity of Triassic fossils from chemosynthetic sites make it difficult to assess the impacts of this directly. Although comprising different tubeworm and mollusc taxa, Mesozoic vent communities largely mirror the diversity of Paleozoic vents (such as when comparing Yaman Kasy and Sibay with Troodos and Figueroa), as well as the observation of the majority of deposits containing only tubeworms. The putative absence of bivalves at Mesozoic vent sites is somewhat puzzling, and may be a result of vent bivalves having occupied habitats away from zones of active mineralisation.

Gastropods and possibly vestimentiferan tubeworms seem to be among the first taxa to colonise vents during the Jurassic, followed by additional gastropod lineages, vent barnacles and alvinellid annelids (from molecular evidence). Vestimentiferans capable of colonising more than one chemosynthetic habitat type appear to have evolved first (Li et al., 2015), suggesting that vestimentiferans may have moved from seeps into vents. Alvinellids do not occupy other chemosynthetic environments such as seeps, and thus may have adapted directly to vent conditions. Throughout the Mesozoic and Cenozoic, a variety of metazoan lineages previously not adapted to vents colonised these environments, indicating that the pull factors of high productivity greatly exceed the costs to adapting to unstable thermal and chemical regimes. The ages of vents within particular geological settings also vary, with back-arc basins being much shorter-lived in comparison to mid-ocean ridges (Woodcock, 2004), and thus new vent habitat generated in association with oceanic arcs may also act to promote vent colonisation by previously non-vent lineages.

Despite a large increase of known vent fossil sites since the last reviews (Little et al., 1998; Campbell, 2006), large knowledge gaps in the understanding of ancient vent communities remain, and uncovering new fossil evidence to fill these is essential. The challenge will be to find ancient examples that are both prospective in terms of palaeo-environment and in terms of preservation. Targeting ancient VMS and SEDEX deposits that have undergone limited metamorphosis is a good starting point. Drillcore archives of mining operations provide samples of inaccessible deposits, that can be used to firstly assess palaeo-oceanographic conditions and their potential to host vent fossils. Projects that focus on finding new VMS-sized mineral resources on the modern ocean floor may also provide drillcore material of Cenozoic-Mesozoic vents, which could also be carefully examined for fossils. In addition to preservation biases at the vent-deposit scale, it is also vital to consider that the vent fossil record is biased towards taxa that possess hard protective structures. Fossilisation studies within modern vent settings can prove very helpful in this respect, as these can be used to quantify how much of the diversity within modern vent sites is not captured within the fossil record. Molecular phylogenetics also forms an important complement to the examination of fossils, and highlights the

interdisciplinary nature of research into ancient vent communities, that provides opportunity for collaboration between mining companies, ore geologists, mineralogists, palaeontologists, molecular and deep-sea biologists.

7 Conclusions

Given the improbability of the mineralisation of animal structures at vent sites, their incorporation into a vent deposit, the preservation of a specific vent deposit into the rock record (rather than it being subducted), as well as that particular vent deposit escaping geological overprinting and later evading destruction during mining activity, it is a wonder that vent fossils exist at all. Vent fossils are relatively rare in comparison to fossils from more typical depositional settings, but despite their scarcity have yielded invaluable insights into the history of life within some of the most fascinating environments on Earth. Hydrothermal vent environments have clearly played an important part in shaping the evolution of life on Earth, acting as incubators of evolutionary novelty that promoted the development of innovative adaptations in deep-sea fauna, to a life fuelled by chemosynthesis in a habitat subjected to unstable chemical and thermal regimes. The unique pathways that evolution has followed under vent conditions presents a strong case for the conservation of modern vent communities, and continued exploration of their evolutionary history.

Acknowledgements

This study was supported by the United Kingdom Natural Environment Research Council (grant to Adrian Glover, number NE/R000670/1), and partly by the South Urals Federal Research Center of Mineralogy and Geoecology UB RAS (state contract AAAA-A19-119061790049-3). We are grateful to everyone who helped in our search for ancient vent fossils, and especially to: Igor G. Zhukov and Alexandr Tseluyko, South Urals Federal Research Center of Mineralogy and Geoecology; Steve Richardson and Andrew McNeill, Mineral Resources Tasmania; Ross Large, University of Tasmania; Tor Grenne, Norges Geologiske Undersøkelse; Steve Piercey, Memorial University; and Stefanie Lode, Geological Survey of Denmark and Greenland.

References

Akahane, H., Furuno, T., Miyajima, H., Yoshikawa, T., Yamamoto, S., 2004. Rapid wood silicification in hot spring water: an explanation of silicification of wood during the Earth's history. Sediment. Geol. 169, 219–228.

Alt, J.C., France-Lanord, C., Floyd, P.A., Castillo, P., Galy, A., 1992. Low temperature hydrothermal alteration of Jurassic ocean crust, site 801. Proc. Ocean Drill. Program, Sci. Results 129, 415–427.

Avdonin, V.V., Sergeeva, N.E., 2020. The relics of hydrothermal fauna in the massive sulfide ores of the VMS deposits of Leninogorsk ore region (Rudny Altai), in: Proceedings of the International Scientific and Practical Conference "Interdisciplinarity of Scientific Research as a Factor of Innovative Development" Vol. 1. OMEGA Science, Yekaterinburg, pp. 28-32 (in Russian).

Avdonin, V.V., Sergeeva, N.E., 2017. The relics of the hydrothermal fauna in the massive sulfide ores of the Gayskoe deposit, in: Proceedings of the International Scientific and Practical Conference "The Interaction of Science and Society: Problems and Prospects" Vol. 3. OMEGA Science, Ufa, pp. 3-5 (in Russian).

Ayupova, N.R., Maslennikov, V. V., 2013. Biomorphic textures in the ferruginous-siliceous rocks of massive sulfide-bearing paleohydrothermal fields in the urals. Lithol. Miner. Resour. 48, 438–455. https://doi.org/10.1134/S0024490213030024

Ayupova, N.R., Maslennikov, V.V., Tessalina, S.G., Shilovsky, O.P., Sadykov, S.A., Hollis, S.P., Danyushevsky, L.V., Safina, N.P., Statsenko, E.O., 2017. Tube fossils from gossanites of the Urals VHMS deposits, Russia: Authigenic mineral assemblages and trace element distributions. Ore Geol. Rev. 85, 107–130. https://doi.org/10.1016/j.oregeorev.2016.08.003

Banks, D.A., 1985. A fossil hydrothermal worm assemblage from the Tynagh lead–zinc deposit in Ireland. Nature 313, 128–131.

Benton, M.J., Harper, D.A., 2020. Introduction to paleobiology and the fossil record. John Wiley & Sons.

Bhaud, M.R., 1998. Species of Spiochaetopterus (Polychaeta, Chaetopteridae) in the Atlantic-Mediterranean biogeographic area. Sarsia 83, 243–263. https://doi.org/10.1080/00364827.1998.10413685

Blumenberg, M., Seifert, R., Buschmann, B., Kiel, S., Thiel, V., 2012. Biomarkers reveal diverse microbial communities in black smoker sulfides from turtle pits (Mid-Atlantic Ridge, Recent) and Yaman Kasy (Russia, Silurian). Geomicrobiol. J. 29, 66–75.

Boirat, J.M., Fouquet, Y., 1986. Decouverte de tubes de vers hydrothermaux fossils dans un amas sulfure de l'Eocene superieur (Barlo, ophiolite de Zambales, Philippines). Comptes Rendue, Ser. II 302, 941–946.

Boyce, A.J., Little, C.T.S., Russel, M.J., 2003. A new fossil vent biota in the Ballynoe barite deposit, Silvermines, Ireland: evidence for intracratpnic sea-floor hydrothermal activity about 352 Ma. Econ. Geol. 98, 649–656.

Brennecka, G.A., Herrmann, A.D., Algeo, T.J., Anbar, A.D., 2011. Rapid expansion of oceanic anoxia immediately before the end-Permian mass extinction. Proc. Natl. Acad. Sci. 108, 17631–17634. https://doi.org/10.1073/pnas.1106039108

Breusing, C., Johnson, S.B., Tunnicliffe, V., Clague, D.A., Vrijenhoek, R.C., Beinart, R.A., 2020. Allopatric and sympatric drivers of speciation in Alviniconcha hydrothermal vent snails. Mol. Biol. Evol. https://doi.org/10.1093/molbev/msaa177

Briggs, D.E.G., Bottrell, S.H., Raiswell, R., 1991. Pyritization of soft-bodied fossils: Beecher's Trilobite Bed, Upper Ordovician, New York State. Geology 19, 1221–1224. https://doi.org/10.1130/0091-7613(1991)019<1221

Briggs, D.E.G., Raiswell, R., Bottrell, S.H., Hatfield, D.T., Bartels, C., 1996. Controls on the pyritization of exceptionally preserved fossils; an analysis of the Lower Devonian Hunsrueck Slate of Germany. Am. J. Sci. 296, 633–663.

Brown, D., Herrington, R.J., Alvarez-Marron, J., 2011. Processes of Arc–Continent Collision in the Uralides. pp. 311–340. https://doi.org/10.1007/978-3-540-88558-0_11

Brown, D., Spadea, P., Puchkov, V., Alvarez-Marron, J., Herrington, R., Willner, A.P., Hetzel, R., Gorozhanina, Y., Juhlin, C., 2006. Arc–continent collision in the Southern Urals. Earth-Science Rev. 79, 261–287. https://doi.org/10.1016/j.earscirev.2006.08.003

Bujtor, L., 2007. A unique Valanginian paleoenvironment at an iron ore deposit near Zengővárkony (Mecsek Mts, South Hungary), and a possible genetic model. Cent. Eur. Geol. 50, 183–198. https://doi.org/10.1556/CEuGeol.50.2007.3.1

939 Bujtor, L., 2006. Early Valanginian brachiopods from the Mecsek Mts. (southern Hungary) and their
940 palaeobiogeographical significance. Neues Jahrb. für Geol. und Paläontologie - Abhandlungen 241,
941 111–152. https://doi.org/10.1127/njgpa/241/2006/111
942 Bujtor, L., Vörös, A., 2020. New kingenoid (Terebratellidina) brachiopods with larger body sizes from the
943 Early Cretaceous of Zengővárkony (Mecsek Mountains, Hungary). J. Paleontol. 94, 475–488.
944 https://doi.org/10.1017/jpa.2019.94
945 Buschmann, B., Maslennikov, V.V., 2006. The late Ordovican or earliest Silurian hydrothermal vent fauna
946 from Yaman Kasy VMS deposit (South Uralides, Russia). Freib. Forschungshefte 14, 139–172.
947 Butterfield, N.J., 2015. Early evolution of the Eukaryota. Palaeontology 58, 5–17.
948 https://doi.org/10.1111/pala.12139
949 Campbell, B., Stein, J., Cary, S., 2003. Evidence of chemolithoautotrophy in the baterial community
950 associated with Alvinella pompejana, a hydrothermal vent polychaete. Appl. Environ. Microbiol. 69,
951 5070– 5078.
952 Campbell, K.A., 2006. Hydrocarbon seep and hydrothermal vent paleoenvironments and paleontology:
953 Past developments and future research directions. Palaeogeogr. Palaeoclimatol. Palaeoecol. 232,
954 362–407. https://doi.org/10.1016/j.palaeo.2005.06.018
955 Chan, C.S., Emerson, D., Luther, G.W., 2016a. The role of microaerophilic Fe-oxidizing micro-organisms
956 in producing banded iron formations. Geobiology 14, 509–528. https://doi.org/10.1111/gbi.12192
957 Chan, C.S., Fakra, S.C., Emerson, D., Fleming, E.J., Edwards, K.J., 2011. Lithotrophic iron-oxidizing
958 bacteria produce organic stalks to control mineral growth: implications for biosignature formation.
959 ISME J. 5, 717–727. https://doi.org/10.1038/ismej.2010.173
960 Chan, C.S., McAllister, S.M., Leavitt, A.H., Glazer, B.T., Krepski, S.T., Emerson, D., 2016b. The
961 architecture of iron microbial mats reflects the adaptation of chemolithotrophic iron oxidation in
962 freshwater and marine environments. Front. Microbiol. 7, 796.
963 https://doi.org/10.3389/fmicb.2016.00796
964 Chen, Y., Niu, Y., Shen, F., Gao, Y., Wang, X., 2020. New U-Pb zircon age and petrogenesis of the
965 plagiogranite, Troodos ophiolite, Cyprus. Lithos 362–363, 105472.
966 https://doi.org/10.1016/j.lithos.2020.105472
967 Chen, Z.-Q., Benton, M.J., 2012. The timing and pattern of biotic recovery following the end-Permian

968 mass extinction. Nat. Geosci. 5, 375–383. https://doi.org/10.1038/ngeo1475
969 Cook, T., Stakes, D., 1995. Biogeological mineralization in deep-sea hydrothermal deposits. Science (80-
970 .). 267, 1975–1979.
971 Corliss, J., Dymond, J., Gordon, L., Edmond, J., von Herzen, R., Ballard, R., Green, K., Williams, D.,
972 Bainbridge, A., Crane, K., van Andel, T., 1979. Submarine thermal springs on the Galapagos Rift.
973 Science (80-.). 203, 1073–1083.
974 Davis, R.E., Stakes, D.S., Wheat, C.G., Moyer, C.L., 2009. Bacterial variability within an iron-silica-
975 manganese-rich hydrothermal mound located off-axis at the Cleft Segment, Juan de Fuca Ridge.
976 Geomicrobiol. J. 26, 570–580. https://doi.org/10.1080/01490450902889080
977 Davison, G.J., Stolz, A.J., Eggins, S.M., 2001. Geochemical anatomy of silica iron exhalites: evidence for
978 hydrothermal oxyanion cycling in response to vent fluid redox and thermal evolution (Mt. Windsor
979 subprovince, Australia). Econ. Geol. 96, 1201–1226.
980 Deamer, D.W., Georgiou, C.D., 2015. Hydrothermal conditions and the origin of cellular life. Astrobiology
981 15, 1091–1095. https://doi.org/10.1089/ast.2015.1338
982 Desbruyères, D., Segonzac, M., Bright, M., 2006. Handbook of deep-sea hydrothermal vent fauna.
983 Ifremer.
984 Dodd, M.S., Papineau, D., Grenne, T., Slack, J.F., Rittner, M., Pirajno, F., O'Neil, J., Little, C.T.S., 2017.
985 Evidence for early life in Earth's oldest hydrothermal vent precipitates. Nature 543, 60–64.
986 https://doi.org/10.1038/nature21377
987 Doyle, M.G., Allen, R.L., 2003. Subsea-floor replacement in volcanic-hosted massive sulfide deposits.
988 Ore Geol. Rev. 23, 183–222. https://doi.org/10.1016/S0169-1368(03)00035-0
989 Dubilier, N., Bergin, C., Lott, C., 2008. Symbiotic diversity in marine animals: the art of harnessing
990 chemosynthesis. Nat. Rev. Microbiol. 6, 725–740. https://doi.org/10.1038/nrmicro1992
991 Duhig, N.C., Davidson, G.J., Stolz, J., 1992a. Microbial involvement in the formation of Cambrian sea-
992 floor silica–iron oxide deposits, Australia. Geology 20, 511–514.
993 Duhig, N.C., Stolz, J., Davidson, G.J., Large, R.R., 1992b. Cambrian microbial and silica gel textures in
994 silica iron exhalites from the Mount Windsor volcanic belt, Australia: their petrography, chemistry,
995 and origin. Econ. Geol. 87, 764–784.
996 Duperron, S., De Beer, D., Zbinden, M., Boetius, A., Schipani, V., Kahil, N., Gaill, F., 2009. Molecular

997 characterization of bacteria associated with the trophosome and the tube of Lamellibrachia sp., a
998 siboglinid annelid from cold seeps in the eastern Mediterranean. FEMS Microbiol. Ecol. 69, 395–
999 409. https://doi.org/10.1111/j.1574-6941.2009.00724.x
1000 Emerson, D., Rentz, J.A., Lilburn, T.G., Davis, R.E., Aldrich, H., Chan, C., Moyer, C.L., 2007. A novel
1001 lineage of Proteobacteria involved in formation of marine Fe-oxidizing microbial mat communities.
1002 PLoS One 2, e667. https://doi.org/10.1371/journal.pone.0000667
1003 Fleming, E.J., Davis, R.E., McAllister, S.M., Chan, C.S., Moyer, C.L., Tebo, B.M., Emerson, D., 2013.
1004 Hidden in plain sight: discovery of sheath-forming, iron-oxidizing Zetaproteobacteria at Loihi
1005 Seamount, Hawaii, USA. FEMS Microbiol. Ecol. 85, 116–127. https://doi.org/10.1111/1574-
1006 6941.12104
1007 Fortey, R., 2000. Olenid trilobites: the oldest known chemoautotrophic symbionts? Proc. Natl. Acad. Sci.
1008 97, 6574–6578. https://doi.org/10.1073/pnas.97.12.6574
1009 Franklin, J.M., Gibson, H.L., Jonasson, I.R., Galley, A.G., 2005. Volcanogenic massive sulfide deposits,
1010 in: Hedenquist, J.W., Thompson, J.F.H., Goldfarb, R.J., Richards, J.P. (Eds.), Economic Geology
1011 100th Anniversary Volume. Society of Economic Geologists, pp. 523–560.
1012 Franklin, J.M., Lydon, J.W., Sangster, D.F., 1981. Volcanic-associated massive sulfide deposits. Econ.
1013 Geol. 75th Anniv. Vol. 485–627.
1014 Galley, A.G., Hannington, M.D., Jonasson, I.R., 2007. Volcanogenic massive sulphide deposits, in:
1015 Goodfellow, W.D. (Ed.), Mineral Deposits of Canada: A Synthesis of Major Deposit-Types, District
1016 Metallogeny, the Evolution of Geological Provinces, and Exploration Methods. Geological
1017 Association of Canada, Mineral Deposits Division, Special Publication No. 5, pp. 141–161.
1018 Georgieva, M.N., 2016. Tube-building annelids from hydrothermal vents and cold seeps: Tube
1019 morphology, fossilisation, and evolutionary history. University of Leeds.
1020 Georgieva, M.N., Little, C.T.S., Bailey, R.J., Ball, A.D., Glover, A.G., 2018. Microbial-tubeworm
1021 associations in a 440 million year old hydrothermal vent community. Proc. R. Soc. B Biol. Sci. 285,
1022 20182004. https://doi.org/10.1098/rspb.2018.2004
1023 Georgieva, M.N., Little, C.T.S., Ball, A.D., Glover, A.G., 2015. Mineralization of Alvinella polychaete tubes
1024 at hydrothermal vents. Geobiology 13, 152–169. https://doi.org/10.1111/gbi.12123
1025 Georgieva, M.N., Little, C.T.S., Watson, J.S., Sephton, M.A., Ball, A.D., Glover, A.G., 2017. Identification

of fossil worm tubes from Phanerozoic hydrothermal vents and cold seeps. J. Syst. Palaeontol. 1–43. https://doi.org/10.1080/14772019.2017.1412362

German, C.R., Petersen, S., Hannington, M.D., 2016. Hydrothermal exploration of mid-ocean ridges: Where might the largest sulfide deposits be forming? Chem. Geol. 420, 114–126. https://doi.org/10.1016/j.chemgeo.2015.11.006

Glasby, G.P., Prozherova, I.A., Maslennikov, V. V., Petukhov, S.I., 2007. Jusa and Barsuchi Log volcanogenic massive sulfide deposits from the Southern Urals of Russia: tectonic setting, structure and mode of formation. Resour. Geol. 57, 24–36. https://doi.org/10.1111/j.1751-3928.2006.00002.x

Grenne, T., Slack, J.F., 2003. Bedded jaspers of the Ordovician Løkken ophiolite, Norway: seafloor deposition and diagenetic maturation of hydrothermal plume-derived silica-iron gels. Miner. Depos. 38, 625–639. https://doi.org/10.1007/s00126-003-0346-3

Gurvich, E.G., 2006. Metalliferous Sediments of the World Ocean: fundamental theory of deep sea hydrothermal sedimentation. Springer, Berlin/Heidelberg. https://doi.org/10.1007/3-540-30969-1

Gusev, G.S., Gushchin, A.. V., Zaykov, V.V., Maslennikov, V.V., Mezhelovsky, N.V., Perevozchikov, B.V., Surin, T.N., Filatov, E.I., Shirai, E.P., 2000. Geology and metallogeny of island arcs, in: Mezhelovsky, N.V., Morozov, A.F., Gusev, G.S., Popov, V.S. (Eds.), Geodynamics and Metallogeny: Theory and Implications for Applied Geology. Inter-Regional Center for Geological Cartography (GEOKART), Ministry of Natural Resources of the Russian Federation, Moscow, pp. 315–337.

Hannington, M., Jamieson, J., Monecke, T., Petersen, S., Beaulieu, S., 2011. The abundance of seafloor massive sulfide deposits. Geology 39, 1155–1158. https://doi.org/10.1130/G32468.1

Hannington, M.D., de Ronde, C.D., Petersen, S., 2005. Sea-floor tectonics and submarine hydrothermal systems. Econ. Geol. 100th Anniv. Vol. 111–141.

Haymon, R., Koski, R., 1985. Evidence of an ancient hydrothermal vent community: fossil worm tubes in Cretaceous sulfide deposits of the Samail Ophiolite, Oman. Bull. Biol. Soc. Washingt. 6, 57–65.

Haymon, R.M., Kastner, M., 1981. Hot spring deposits on the East Pacific Rise at 21°N: preliminary description of mineralogy and genesis. Earth Planet. Sci. Lett. 53, 363–381.

Haymon, R.M., Koski, R.A., Sinclair, C., 1984. Fossils of hydrothermal vent worms from Cretaceous sulfide ores of the Samail Ophiolite, Oman. Science (80-.). 223, 1407–1409.

1055 Herrera, S., Watanabe, H., Shank, T.M., 2015. Evolutionary and biogeographical patterns of barnacles
1056 from deep-sea hydrothermal vents. Mol. Ecol. 24, 673–689. https://doi.org/10.1111/mec.13054
1057 Herrington, R.J., Armstrong, R.N., Zaykov, V. V., Maslennikov, V. V., Tessalina, S.G., Orgeval, J.-J.,
1058 Taylor, R.N.A., 2002. Massive sulfide deposits in the south Urals: Geological setting within the
1059 framework of the Uralide orogen, in: Brown, D., Juhlin, C., Puchkov, V. (Eds.), Mountain Building in
1060 the Uralides: Pangea to the Present. American Geophysical Union, Washington, D. C., pp. 155–
1061 182. https://doi.org/10.1029/132GM09
1062 Herrington, R.J., Maslennikov, V. V., Brown, D., Puchkov, V.N., 2005a. Mineral deposits of the Urals and
1063 links to geodynamic evolution. Econ. Geol. 100th Anniv. Vol. 1069–1095.
1064 Herrington, R.J., Maslennikov, V. V., Spiro, B., Zaykov, V. V., Little, C.T.S., 1998. Ancient vent chimney
1065 structures in the Silurian massive sulphides of the Urals., in: Mills, R.A., Harrison, K. (Eds.), Modern
1066 Ocean Floor Processes and the Geological Record. Special Publication of the Geological Society,
1067 London, pp. 241–258.
1068 Herrington, R.J., Maslennikov, V. V., Zaykov, V., Seravkin, I., Kosarev, A., Buschmann, B., Orgeval, J.-J.,
1069 Holland, N., Tesalina, S., Nimis, P., Armstrong, R., 2005b. 6: Classification of VMS deposits: lessons
1070 from the South Uralides. Ore Geol. Rev. 27, 203–237.
1071 https://doi.org/10.1016/j.oregeorev.2005.07.014
1072 Herrington, R.J., Puchkov, V.N., Yakubchuk, A.S., 2005c. A reassessment of the tectonic zonation of the
1073 Uralides: implications for metallogeny. Geol. Soc. London, Spec. Publ. 248, 153–166.
1074 https://doi.org/10.1144/GSL.SP.2005.248.01.08
1075 Hilário, A., Capa, M., Dahlgren, T.G., Halanych, K.M., Little, C.T.S., Thornhill, D.J., Verna, C., Glover,
1076 A.G., 2011. New perspectives on the ecology and evolution of siboglinid tubeworms. PLoS One 6,
1077 e16309. https://doi.org/10.1371/journal.pone.0016309
1078 Huston, D.L., Eglington, B.M., Pehrsson, S., Piercey, S.J., 2015. The metallogeny of zinc through time:
1079 links to secular changes in the atmosphere, hydrosphere, and the supercontinent cycle, in:
1080 Archibald, S.M., Piercey, S.J. (Eds.), Current Perspectives on Zinc Deposits. Irish Association for
1081 Economic Geology Special Publication on Zinc Deposits, pp. 1–16.
1082 Huston, D.L., Pehrsson, S., Eglington, B.M., Zaw, K., 2010. The geology and metallogeny of volcanic-
1083 hosted massive sulfide deposits: variations through geologic time and with tectonic setting. Econ.

Geol. 105, 571–591. https://doi.org/10.2113/gsecongeo.105.3.571

Ivanov, S.N., 1959. Discussion of some modern question of the genesis of the Uralian massive sulphide deposits. Publ. Mining-Geology Inst. 43, 7–78.

Ivanov, S.N., 1947. Study experience of geology and mineralogy of the Sibay massive sulphide deposit. Akad. Nauk SSSR, Ural. Fil. 2, 1-109 (in Russian).

Johannessen, K.C., Vander Roost, J., Dahle, H., Dundas, S.H., Pedersen, R.B., Thorseth, I.H., 2017. Environmental controls on biomineralization and Fe-mound formation in a low-temperature hydrothermal system at the Jan Mayen Vent Fields. Geochim. Cosmochim. Acta 202, 101–123. https://doi.org/10.1016/j.gca.2016.12.016

Jones, B., Renaut, R.W., 2003. Hot spring and geyser sinters: the integrated product of precipitation, replacement, and deposition. Can. J. Earth Sci. 40, 1549–1569. https://doi.org/10.1139/e03-078

Juniper, S.K., Fouquet, Y., 1988. Filamentous iron-silica deposits from modern and ancient hydrothermal sites. Can. Mineral. 26, 859–869.

Kaim, A., Jenkins, R.G., Tanabe, K., Kiel, S., 2014. Mollusks from late Mesozoic seep deposits, chiefly in California. Zootaxa 3861, 401–440.

Kennett, J.P., Stott, L.D., 1991. Abrupt deep-sea warming, palaeoceanographic changes and benthic extinctions at the end of the Palaeocene. Nature 353, 225–229. https://doi.org/10.1038/353225a0

Kiel, S., 2016. A biogeographic network reveals evolutionary links between deep-sea hydrothermal vent and methane seep faunas. Proc. R. Soc. B Biol. Sci. 283, 20162337. https://doi.org/10.1098/rspb.2016.2337

Kiel, S., Dando, P.R., 2009. Chaetopterid tubes from vent and seep sites: implications for fossil record and evolutionary history of vent and seep annelids. Acta Palaeontol. Pol. 54, 443–448. https://doi.org/10.4202/app.2009.0022

Kiel, S., Little, C.T.S., 2006. Cold-seep mollusks are older than the general marine mollusk fauna. Science (80-.). 313, 1429–1431. https://doi.org/10.1126/science.1126286

Knoll, A.., Javaux, E.., Hewitt, D., Cohen, P., 2006. Eukaryotic organisms in Proterozoic oceans. Philos. Trans. R. Soc. B Biol. Sci. 361, 1023–1038. https://doi.org/10.1098/rstb.2006.1843

Koschinsky, A., Garbe-Schönberg, D., Sander, S., Schmidt, K., Gennerich, H.-H., Strauss, H., 2008. Hydrothermal venting at pressure-temperature conditions above the critical point of seawater, 5°S

on the Mid-Atlantic Ridge. Geology 36, 615. https://doi.org/10.1130/G24726A.1

Kumar, S., 2005. Molecular clocks: four decades of evolution. Nat. Rev. Genet. 6, 654–662. https://doi.org/10.1038/nrg1659

Kuznetsov, A.P., Maslennikov, V. V., Zaikov, V. V., 1993. The near-hydrothermal fauna of the Silurian paleoocean in the south Ural. Izv. Akad. Nauk SSSR, Seriya Biol. 4, 525–534.

Kuznetsov, A.P., Maslennikov, V. V., Zaikov, V. V., Sobetskii, V.A., 1988. Fossil fauna in the sulfide hydrothermal hills from the middle Devonian paleo-ocean of the Ural area. Dokl. Akad. Nauk SSSR 303, 1477–1481.

Kuznetsov, A.P., Maslennikov, V. V., Zaikov, V. V., Zonenshain, L.P., 1991a. Fossil hydrothermal vent fauna in Devonian sulfide deposits of the Uralian ophiolites. Deep Sea Newsl. 17, 9–11.

Kuznetsov, A.P., Zaikov, V. V., Maslennikov, V. V., 1991b. Ophiolites, the “chronicle” of volcanic, tectonic, physical, chemical and biotic earth crust formation events on the paleoocean bottom. Izv. Akad. Nauk SSSR, Seriya Biol. 2.

Lalou, C., 1991. Deep-sea hydrothermal venting: a recently discovered marine system. J. Mar. Syst. 1, 403–440. https://doi.org/10.1016/0924-7963(91)90007-H

Laznicka, P., 2010. Oceans and young island arc systems, in: Giant Metallic Deposits. Springer Berlin Heidelberg, Berlin, Heidelberg, pp. 81–108. https://doi.org/10.1007/978-3-642-12405-1_5

Leach, D., Marsh, E., Bradley, D., Gardoll, S., Huston, D., 2005. The distribution of SEDEX Pb-Zn deposits through Earth history, in: Mineral Deposit Research: Meeting the Global Challenge. Springer Berlin Heidelberg, Berlin, Heidelberg, pp. 145–148. https://doi.org/10.1007/3-540-27946-6_38

Lepot, K., 2020. Signatures of early microbial life from the Archean (4 to 2.5 Ga) eon. Earth-Science Rev. 209, 103296. https://doi.org/10.1016/j.earscirev.2020.103296

Li, J., Kusky, T.M., 2007. World’s largest known Precambrian fossil black smoker chimneys and associated microbial vent communities, North China: Implications for early life. Gondwana Res. 12, 84–100. https://doi.org/10.1016/j.gr.2006.10.024

Li, Y., Kocot, K.M., Schander, C., Santos, S.R., Thornhill, D.J., Halanych, K.M., 2015. Mitogenomics reveals phylogeny and repeated motifs in control regions of the deep-sea family Siboglinidae (Annelida). Mol. Phylogenet. Evol. 85, 221–229. https://doi.org/10.1016/j.ympev.2015.02.008

Li, Y., Tassia, M.G., Waits, D.S., Bogantes, V.E., David, K.T., Halanych, K.M., 2019. Genomic adaptations to chemosymbiosis in the deep-sea seep-dwelling tubeworm Lamellibrachia luymesi. BMC Biol. 17, 91. https://doi.org/10.1186/s12915-019-0713-x

Little, C.T.S., 2009. Hot stuff in the deep sea. Planet Earth.

Little, C.T.S., Cann, J.R., Herrington, R.J., Morisseau, M., 1999a. Late Cretaceous hydrothermal vent communities from the Troodos ophiolite, Cyprus. Geology 27, 1027–1030.

Little, C.T.S., Danelian, T., Herrington, R., Haymon, R., 2004a. Early Jurassic hydrothermal vent community from the Franciscan Complex, California. J. Paleontol. 78, 542–559.

Little, C.T.S., Glynn, S.E.J., Mills, R.A., 2004b. Four-hundred-and-ninety-million-year record of bacteriogenic iron oxide precipitation at sea-floor hydrothermal vents. Geomicrobiol. J. 21, 415–429. https://doi.org/10.1080/01490450490485845

Little, C.T.S., Herrington, R.J., Haymon, R.M., Danelian, T., 1999b. Early Jurassic hydrothermal vent community from the Franciscan Complex, San Rafael Mountains, California. Geology 27, 167–170.

Little, C.T.S., Herrington, R.J., Maslennikov, V. V., Morris, N.J., Zaykov, V. V., 1997. Silurian hydrothermal-vent community from the southern Urals, Russia. Nature 385, 146–148. https://doi.org/10.1038/385146a0

Little, C.T.S., Herrington, R.J., Maslennikov, V.V., Zaykov, V.V., 1998. The fossil record of hydrothermal vent communities. Geol. Soc. London, Spec. Publ. 148, 259–270. https://doi.org/10.1144/GSL.SP.1998.148.01.14

Little, C.T.S., Johannessen, K.C., Bengtson, S., Chan, C.S., Ivarsson, M., Slack, J.F., Broman, C., Thorseth, I.H., Grenne, T., Rouxel, O.J., Bekker, A., 2021. A late Paleoproterozoic (1.74 Ga) deep-sea, low-temperature, iron-oxidizing microbial hydrothermal vent community from Arizona, USA. Geobiology gbi.12434. https://doi.org/10.1111/gbi.12434

Little, C.T.S., Magalashvili, A., Banks, D., 2007. Neotethyan Late Cretaceous volcanic arc hydrothermal vent fauna. Geology 35, 835–838.

Little, C.T.S., Maslennikov, V. V, Morris, N.J., Gubanov, A.P., 1999c. Two Palaeozoic hydrothermal vent communities from the southern Ural mountains, Russia. Palaeontology 42, 1043–1078.

Little, C.T.S., Vrijenhoek, R.C., 2003. Are hydrothermal vent animals living fossils? Trends Ecol. Evol. 18, 582–588. https://doi.org/10.1016/j.tree.2003.08.009

Lode, S., Georgieva, M.N., Little, C.T.S., Herrington, R.J., Piercey, S.J., 2020. A glimpse into ~500-million-year-old hydrothermal vent biology: Insights from biogenic textures recorded within Cambrian hydrothermal mudstones of central Newfoundland, Canada. in prep.

Lode, S., Piercey, S.J., Layne, G.D., Piercey, G., Cloutier, J., 2016. Multiple sulphur and lead sources recorded in hydrothermal exhalites associated with the Lemarchant volcanogenic massive sulphide deposit, central Newfoundland, Canada. Miner. Depos. 52, 105–128. https://doi.org/10.1007/s00126-016-0652-1

Logan, G.A., Hinman, M.C., Walter, M.R., Summons, R.E., 2001. Biogeochemistry of the 1640 Ma McArthur River (HYC) lead-zinc ore and host sediments, Northern Territory, Australia. Geochim. Cosmochim. Acta 65, 2317–2336. https://doi.org/10.1016/S0016-7037(01)00599-3

Lonsdale, P., 1977. Clustering of suspension-feeding macrobenthos near abyssal hydrothermal vents at oceanic spreading centers. Deep Sea Res. 24, 857–863.

Lopez-Garcia, P., Gaill, F., Moreira, D., 2002. Wide bacterial diversity associated with tubes of the vent worm Riftia pachyptila. Environ. Microbiol. 4, 204–215. https://doi.org/10.1046/j.1462-2920.2002.00286.x

Lorion, J., Kiel, S., Faure, B., Kawato, M., Ho, S.Y.W., Marshall, B., Tsuchida, S., Miyazaki, J.-I., Fujiwara, Y., 2013. Adaptive radiation of chemosymbiotic deep-sea mussels. Proc. R. Soc. B Biol. Sci. 280, 1243. https://doi.org/10.1098/rspb.2013.1243

Louca, S., Pennell, M.W., 2020. Extant timetrees are consistent with a myriad of diversification histories. Nature 580, 502–505. https://doi.org/10.1038/s41586-020-2176-1

Maginn, E.J., Little, C.T.S., Herrington, R.J., Mills, R.A., 2002. Sulphide mineralisation in the deep sea hydrothermal vent polychaete, Alvinella pompejana: implications for fossil preservation. Mar. Geol. 181, 337–356.

Martin, W., Baross, J., Kelley, D., Russell, M.J., 2008. Hydrothermal vents and the origin of life. Nat. Rev. Microbiol. 6, 805–814. https://doi.org/10.1038/nrmicro1991

Maslennikov, V. V., 1999. Sedimentohenesis, hamyrolysis and ecology of the massive sulfide-bearing paleohydrothermal fields (South Urals example) (in Russian). Geotur, Miass.

Maslennikov, V. V., 1991. The Lithological Control of Copper-Pyritic Ores (by Example of Sibay and Oko'abrsk Deposits of Ural). Urals Branch of the Science Academy of USSR, Sverdlovsk (in

Russian).

Maslennikov, V. V., Ayupova, N.R., Maslennikova, S.P., Lein, A.Y., Tseluiko, A.S., Danyushevsky, L. V., Large, R.R., Simonov, V.A., 2017. Criteria for the detection of hydrothermal ecosystem faunas in ores of massive sulfide deposits in the Urals. Lithol. Miner. Resour. 52, 173–191. https://doi.org/10.1134/S002449021703004X

Maslennikov, V.V., Ayupova, N.R., Maslennikova, S.P., Tselyiko, A.S., 2016. Hydrothermal biomorphoses of massive sulfide deposits: biomineralization, trace elements, and bio-productivity criteria. RIO UB RAS, Yekaterinburg (in Russian).

McAllister, S.M., Moore, R.M., Gartman, A., Luther, G.W., Emerson, D., Chan, C.S., 2019. The Fe(II)-oxidizing Zetaproteobacteria: historical, ecological and genomic perspectives. FEMS Microbiol. Ecol. 95, fiz015. https://doi.org/10.1093/femsec/fiz015

McGoldrick, P.J., 1999. Northern Australian "SEDEX" Zn–Pb deposits: microbial oases in Proterozoic seas, in: Stanley, C.J. (Ed.), Mineral Deposits: Processes to Processing: Proceedings of the 5th Biennial SGA Meeting. Balkema, Rotterdam, pp. 885–888.

McLean, J.H., 1981. The Galapagos Rift limpet Neomphalus: relevance to understanding the evolution of a major Paleozoic–Mesozoic radiation. Malacologia 11, 291–336.

Mitarai, S., Watanabe, H., Nakajima, Y., Shchepetkin, A.F., McWilliams, J.C., 2016. Quantifying dispersal from hydrothermal vent fields in the western Pacific Ocean. Proc. Natl. Acad. Sci. 113, 2976–2981. https://doi.org/10.1073/pnas.1518395113

Moore, D.W., Young, L.E., Modene, J.S., Plahuta, J.T., 1986. Geologic setting and genesis of the Red Dog zinc–lead–silver deposit, western Brooks Range, Alaska. Econ. Geol. 81, 1696–1727.

Morag, N., Golan, T., Katzir, Y., Coble, M.A., Kitajima, K., Valley, J.W., 2020. The origin of plagiogranites: coupled SIMS O isotope ratios, U–Pb dating and trace element composition of zircon from the Troodos Ophiolite, Cyprus. J. Petrol. https://doi.org/10.1093/petrology/egaa057

Morineaux, M., Nishi, E., Ormos, A., Mouchel, O., 2010. A new species of Phyllochaetopterus (Annelida: Chaetopteridae) from deep-sea hydrothermal Ashadze-1 vent field, Mid-Atlantic Ridge: taxonomical description and partial COI DNA sequence. Cah. Biol. Mar. 51, 239–248.

Newman, W.A., 1985. The abyssal hydrothermal vent invertebrate fauna. A glimpse of antiquity? Bull. Biol. Soc. Washingt. 6, 231–242.

Oehler, J.H., Logan, R.G., 1977. Microfossils, cherts, and associated mineralisation in the Proterozoic McArthur (H.Y.C.) lead-zinc-silver deposit. Econ. Geol. 72, 1393–1409.

Okumura, T., Ohara, Y., Stern, R.J., Yamanaka, T., Onishi, Y., Watanabe, H., Chen, C., Bloomer, S.H., Pujana, I., Sakai, S., Ishii, T., Takai, K., 2016. Brucite chimney formation and carbonate alteration at the Shinkai Seep Field, a serpentinite-hosted vent system in the southern Mariana forearc. Geochemistry, Geophys. Geosystems 17, 3775–3796. https://doi.org/10.1002/2016GC006449

Oudin, E., Bouladon, J., Paris, J.P., 1985. Vers hydrothermaux fossils dans une mineralisation sulfuree des ophiolites de Nouvelle–Calédonie. Acad. des Sci. Compte Rendus, Ser. II 301, 157–162.

Oudin, E., Constantinou, G., 1984. Black smoker chimney fragments in Cyprus sulphide deposits. Nature 308, 349–353. https://doi.org/10.1038/308349a0

Peng, X., Zhou, H., Yao, H., Li, J., Wu, Z., 2009. Ultrastructural evidence for iron accumulation within the tube of Vestimentiferan Ridgeia piscesae. Biometals 22, 723–732.

Peng, X., Zhou, H.H., Tang, S., Yao, H., Jiang, L., Wu, Z., 2008. Early-stage mineralization of hydrothermal tubeworms: New insights into the role of microorganisms in the process of mineralization. Chinese Sci. Bull. 53, 251–261. https://doi.org/10.1007/s11434-007-0517-1

Perez, A., Umino, S., Yumul Jr., G.P., Ishizuka, O., 2018. Boninite and boninite-series volcanics in northern Zambales ophiolite: doubly vergent subduction initiation along Philippine Sea plate margins. Solid Earth 9, 713–733. https://doi.org/10.5194/se-9-713-2018

Petersen, S., Krätschell, A., Augustin, N., Jamieson, J., Hein, J.R., Hannington, M.D., 2016. News from the seabed - geological characteristics and resource potential of deep-sea mineral resources. Mar. Policy 70, 175–187. https://doi.org/10.1016/j.marpol.2016.03.012

Playford, P.E., Wallace, M.W., 2001. Exhalative mineralization in Devonian reef complexes of the Canning Basin, Western Australia. Econ. Geol. 96, 1595–1610.

Pradillon, F., Zbinden, M., Le Bris, N., Hourdez, S., Barnay, a.-S., Gaill, F., 2009. Development of assemblages associated with alvinellid colonies on the walls of high-temperature vents at the East Pacific Rise. Deep Sea Res. Part II Top. Stud. Oceanogr. 56, 1622–1631. https://doi.org/10.1016/j.dsr2.2009.05.009

Prokin, V.A., Buslaev, F.P., 1999. Massive copper-zinc sulphide deposits in the Urals. Ore Geol. Rev. 14, 1–69.

Pshenichniy, G.N., 1984. Ore structures and textures from the deposits of the massive sulphide formation of the South Urals. Nauka, Moscow.

Puchkov, V.N., 1997. Structure and geodynamics of the Uralian orogen. Geol. Soc. London, Spec. Publ. 121, 201–236. https://doi.org/10.1144/GSL.SP.1997.121.01.09

Rasmussen, B., 2000. Filamentous microfossils in a 3,235-million-year-old volcanogenic massive sulphide deposit. Nature 405, 676–679.

Revan, M.K., Hisatani, K., Miyamoto, H., Delibaş, O., Hanilçi, N., Aysal, N., Özkan, M., Çolak, T., Karslı, Ş., Peytcheva, I., 2017. Geology, U-Pb geochronology, and stable isotope geochemistry of the Tunca semi-massive sulfide mineralization, Black Sea region, NE Turkey: implications for ore genesis. Ore Geol. Rev. 89, 369–389. https://doi.org/10.1016/j.oregeorev.2017.06.024

Revan, M.K., Unlu, T., Genc, Y., 2010. Preliminary findings on the fossil traces in the massive sulphite deposits of eastern Black Sea region (Lahanos, Killik and Cayeli). Miner. Resour. Exploit. Bull. 140, 73–79.

Reysenbach, A.L., Cady, S.L., 2001. Microbiology of ancient and modern hydrothermal systems. Trends Microbiol. 9, 79–86. https://doi.org/10.1016/S0966-842X(00)01921-1

Robertson, A.H.F., Parlak, O., Ustaömer, T., 2012. Overview of the Palaeozoic–Neogene evolution of Neotethys in the Eastern Mediterranean region (southern Turkey, Cyprus, Syria). Pet. Geosci. 18, 381–404. https://doi.org/10.1144/petgeo2011-091

Roterman, C.N., Lee, W.-K., Liu, X., Lin, R., Li, X., Won, Y.-J., 2018. A new yeti crab phylogeny: vent origins with indications of regional extinction in the East Pacific. PLoS One 13, e0194696. https://doi.org/10.1371/journal.pone.0194696

Rouxel, O., Toner, B., Germain, Y., Glazer, B., 2018. Geochemical and iron isotopic insights into hydrothermal iron oxyhydroxide deposit formation at Loihi Seamount. Geochim. Cosmochim. Acta 220, 449–482. https://doi.org/10.1016/j.gca.2017.09.050

Russell, M.J., Hall, A.J., 1997. The emergence of life from iron monosulphide bubbles at a submarine hydrothermal redox and pH front. J. Geol. Soc. London. 154, 377–402. https://doi.org/10.1144/gsjgs.154.3.0377

Sandy, M.R., 1995. A review of some Palaeozoic and Mesozoic brachiopods as members of cold seep chemosynthetic communities: “unusual” palaeoecology and anomalous palaeobiogeographic

pattern explained. Földtani Közlöny 125, 241–258.

Sanfilippo, R., Rosso, A., Reitano, A., Insacco, G., 2017. First record of sabellid and serpulid polychaetes from the Permian of Sicily. Acta Palaeontol. Pol. 62, 25–38. https://doi.org/10.4202/app.00288.2016

Sasaki, T., Warén, A., Kano, Y., Okutani, T., Fujikura, K., 2010. Gastropods from recent hot vents and cold seeps: systematics, diversity and life strategies, in: Kiel, S. (Ed.), The Vent and Seep Biota. Springer, pp. 169–254. https://doi.org/10.1007/978-90-481-9572-5_7

Searle, M.P., Waters, D.J., Garber, J.M., Rioux, M., Cherry, A.G., Ambrose, T.K., 2015. Structure and metamorphism beneath the obducting Oman ophiolite: Evidence from the Bani Hamid granulites, northern Oman mountains. Geosphere 11, 1812–1836. https://doi.org/10.1130/GES01199.1

Seravkin, I.B., 2010. Metallogeniya Yuzhnogo Urala i Tsentral'nogo Kazakhstana (Metallogeny of the South Urals and Central Kazakhstan). AN RB, Gilem, Ufa.

Shah, D.U., Vollrath, F., Stires, J., Deheyn, D.D., 2015. The biocomposite tube of a chaetopterid marine worm constructed with highly-controlled orientation of nanofilaments. Mater. Sci. Eng. C 48, 408–415. https://doi.org/10.1016/j.msec.2014.12.015

Shpanskaya, A.Y., Maslennikov, V. V., Little, C.T.S., 1999. Vestimnetiferan tubes from the Early Silurian and Middle Devonian hydrothermal biota of the Uralian palaeobasin. Paleontol. Zhurnal 33, 222–228.

Slack, J.F., Grenne, T., Bekker, A., Rouxel, O.J., Lindberg, P.A., 2007. Suboxic deep seawater in the late Paleoproterozoic: evidence from hematitic chert and iron formation related to seafloor-hydrothermal sulfide deposits, central Arizona, USA. Earth Planet. Sci. Lett. 255, 243–256. https://doi.org/10.1016/j.epsl.2006.12.018

Smith, C.R., Glover, A.G., Treude, T., Higgs, N.D., Amon, D.J., 2015. Whale-fall ecosystems: recent insights into ecology, paleoecology, and evolution. Ann. Rev. Mar. Sci. 7, 571–596. https://doi.org/10.1146/annurev-marine-010213-135144

Sogin, E.M., Leisch, N., Dubilier, N., 2020. Chemosynthetic symbioses. Curr. Biol. 30, R1137–R1142. https://doi.org/10.1016/j.cub.2020.07.050

Sugitani, K., Mimura, K., Takeuchi, M., Yamaguchi, T., Suzuki, K., Senda, R., Asahara, Y., Wallis, S., Van Kranendonk, M.J., 2015. A Paleoarchean coastal hydrothermal field inhabited by diverse microbial

communities: the Strelley Pool Formation, Pilbara Craton, Western Australia. Geobiology 13, 522–545. https://doi.org/10.1111/gbi.12150

Sun, J., Zhang, Yu, Xu, T., Zhang, Yang, Mu, H., Zhang, Yanjie, Lan, Y., Fields, C.J., Hui, J.H.L., Zhang, W., Li, R., Nong, W., Cheung, F.K.M., Qiu, J.-W., Qian, P.-Y., 2017. Adaptation to deep-sea chemosynthetic environments as revealed by mussel genomes. Nat. Ecol. Evol. 1, 0121. https://doi.org/10.1038/s41559-017-0121

Sun, S., Sha, Z., Wang, Y., 2018. Phylogenetic position of Alvinocarididae (Crustacea: Decapoda: Caridea): new insights into the origin and evolutionary history of the hydrothermal vent alvinocarid shrimps. Deep Sea Res. Part I Oceanogr. Res. Pap. 141, 93–105. https://doi.org/10.1016/j.dsr.2018.10.001

Sun, Z., Li, Jun, Huang, W., Dong, H., Little, C.T.S., Li, Jiwei, 2015. Generation of hydrothermal Fe-Si oxyhydroxide deposit on the Southwest Indian Ridge and its implication for the origin of ancient banded iron formations. J. Geophys. Res. Biogeosciences 120, 187–203. https://doi.org/10.1002/2014JG002764

Ulrich, M., Picard, C., Guillot, S., Chauvel, C., Cluzel, D., Meffre, S., 2010. Multiple melting stages and refertilization as indicators for ridge to subduction formation: The New Caledonia ophiolite. Lithos 115, 223–236.

Van Dover, C., 2000. The ecology of deep-sea hydrothermal vents. Princeton University Press.

Vander Roost, J., Daae, F.L., Steen, I.H., Thorseth, I.H., Dahle, H., 2018. Distribution patterns of iron-oxidizing Zeta- and Beta-proteobacteria from different environmental settings at the Jan Mayen Vent Fields. Front. Microbiol. 9. https://doi.org/10.3389/fmicb.2018.03008

Vander Roost, J., Thorseth, I.H., Dahle, H., 2017. Microbial analysis of Zetaproteobacteria and co-colonizers of iron mats in the Troll Wall Vent Field, Arctic Mid-Ocean Ridge. PLoS One 12, e0185008. https://doi.org/10.1371/journal.pone.0185008

Vinn, O., Kupriyanova, E.K., Kiel, S., 2013. Serpulids (Annelida, Polychaeta) at Cretaceous to modern hydrocarbon seeps: Ecological and evolutionary patterns. Palaeogeogr. Palaeoclimatol. Palaeoecol. 390, 35–41. https://doi.org/10.1016/j.palaeo.2012.08.003

Von Damm, K.L., Edmond, J.M., Measures, C.I., Grant, B., 1985. Chemistry of submarine hydrothermal solutions at Guaymas Basin, Gulf of California. Geochim. Cosmochim. Acta 49, 2221–2237.

https://doi.org/10.1016/0016-7037(85)90223-6

Vrijenhoek, R.C., 2013. On the instability and evolutionary age of deep-sea chemosynthetic communities. Deep Sea Res. II 92, 189–200. https://doi.org/10.1016/j.dsr2.2012.12.004

Wacey, D., Saunders, M., Cliff, J., Kilburn, M.R., Kong, C., Barley, M.E., Brasier, M.D., 2014. Geochemistry and nano-structure of a putative ~3240 million-year-old black smoker biota, Sulphur Springs Group, Western Australia. Precambrian Res. 249, 1–12. https://doi.org/10.1016/j.precamres.2014.04.016

Weigert, A., Bleidorn, C., 2016. Current status of annelid phylogeny. Org. Divers. Evol. 16, 345–362. https://doi.org/10.1007/s13127-016-0265-7

Weigert, A., Helm, C., Meyer, M., Nickel, B., Arendt, D., Hausdorf, B., Santos, S.R., Halanych, K.M., Purschke, G., Bleidorn, C., Struck, T.H., 2014. Illuminating the base of the annelid tree using transcriptomics. Mol. Biol. Evol. 31, 1391–1401. https://doi.org/10.1093/molbev/msu080

Weiss, M.C., Preiner, M., Xavier, J.C., Zimorski, V., Martin, W.F., 2018. The last universal common ancestor between ancient Earth chemistry and the onset of genetics. PLOS Genet. 14, e1007518. https://doi.org/10.1371/journal.pgen.1007518

Weiss, M.C., Sousa, F.L., Mrnjavac, N., Neukirchen, S., Roettger, M., Nelson-Sathi, S., Martin, W.F., 2016. The physiology and habitat of the last universal common ancestor. Nat. Microbiol. 1, 16116. https://doi.org/10.1038/nmicrobiol.2016.116

Woodcock, N.H., 2004. Life span and fate of basins. Geology 32, 685–688. https://doi.org/10.1130/G20598.1

Yang, R., Wei, H., Bao, M., Wang, W., Wang, Q., Zhang, X., Liu, L., 2008. Discovery of hydrothermal venting community at the base of Cambrian barite in Guizhou Province, Western China: Implication for the Cambrian biological explosion. Prog. Nat. Sci. 18, 65–70. https://doi.org/10.1016/j.pnsc.2007.07.006

Zaykov, V. V., Maslennikov, V. V., Zaykova, E. V., Herrington, R.J., 1996. Hydrothermal activity and segmentation in the Magnitogorsk-West Mugodjarian zone on the margins of the Urals palaeo-ocean. Geol. Soc. London, Spec. Publ. 118, 199–210. https://doi.org/10.1144/GSL.SP.1996.118.01.12

Zaykov, V.V., 2006. Vulkanizm i sul'fidnye kholmy paleookeanicheskikh okrain (Volcanism and Sulfide

Mounds of Paleooceanic Margins). Nauka, Moscow.

Zbinden, M., Martinez, I., Guyot, F., Cambon-Bonavita, M.-A., Gaill, F., 2001. Zinc-iron sulphide mineralization in tubes of hydrothermal vent worms. Eur. J. Mineral. 13, 653–658. https://doi.org/10.1127/0935-1221/2001/0013-0653

Tables

Table 1. Reported fossils from ancient hydrothermal vent deposits. Updated from Little et al. (1998) and Campbell (2006), with fossiliferous vent deposits reported since these reviews highlighted.

#	Deposit name/location	Geo-tectonic/stratigraphic context	Age	Deposit type	Fauna	Inferred paleo-depth/setting	References
1	Barlo, Luzon, Philippines	Supra-subduction zone	Upper Eocene, Zambales Ophiolite	VMS deposit	Vestimentiferan? worm tubes, filaments in jasper	Deep offshore	(Boirat and Fouquet, 1986; Little et al., 1998; Campbell, 2006)
2	Azema, New Caledonia	Oceanic spreading centre	Paleocene or Upper Cretaceous; ophiolite	VMS deposit	Worm tubes	Deep offshore	(Oudin et al., 1985; Little et al., 1998; Campbell, 2006)
3	Madneuli, Georgia	Supra-subduction arc setting	Late Cretaceous	VMS deposit	Worm tubes	Shallow marine	(Little et al., 2007)
4	Lahanos, Killik, Çayeli, Kisilkaya sites, eastern Black Sea, Turkey	Supra-subduction arc setting	Upper Cretaceous	VMS deposits	Worm tubes	-	(Revan et al., 2010; Maslennikov et al., 2016)
5	Kapedhes, Kinousa, Kambia, Memi, Sha, Peristerka sites, Cyprus	Supra-subduction fore-arc setting	Upper Cretaceous, Turonian, Troodos Ophiolite	VMS deposits	Vestimentiferan worm tubes, serpulid? worm tubes, cerithids or provannids, epitoniids, filaments in jasper	Deep offshore	(Oudin and Constantinou, 1984; Little et al., 1998, 1999a)
6	Bayda, Oman	Supra-subduction fore-arc setting	Upper Cretaceous, Cenomanian, Samail Ophiolite	VMS deposit	Vestimentiferan? worm tubes	Deep offshore	(Haymon et al., 1984; Haymon and Koski, 1985; Little et al., 1998; Campbell, 2006)

7	Zengővárkony, Mecsek Mountains, southern Hungary	Rift basin, iron-ore depositional setting linked to former hydrothermal activity on the seafloor	Lower Cretaceous	Iron ore deposit	Brachiopods: *Lacunosella hoheneggeri*, *Nucleata veronica*, *Moutonithyris* aff. *M. moutoniana, Karadagithyris* sp., *Zittelina pinguicula*, *Dictyothyropsis vogli*, *Zittelina hofmanni*, *Smirnovina ferraria*	-	(Bujtor, 2006, 2007; Bujtor and Vörös, 2020)
8	Coast Range Ophiolite, California, USA	Supra-subduction zone fore-arc basin	Late Jurassic	Ophiolite	Filaments in jasper	-	(Juniper and Fouquet, 1988; Little et al., 2004b)
9	OPD Core 129-801C-4R, Pigafetta Basin, W. Pacific	Mid-ocean ridge and ocean island	Mid Jurassic	-	Filaments in jasper	-	(Alt et al., 1992; Little et al., 2004b)
10	Figueroa, San Rafael Mountains, southern California, USA	Mid-ocean ridge or seamount	Lower Jurassic, Pleinsbachian, Franciscan Complex	VMS deposit	Vestimentiferan worm tubes, *Anarhynchia gabbi*, *Francisciconcha maslennikovi*, filaments in jasper	cf.Deep offshore	(Little et al., 1999b, 2004a; Campbell, 2006)
11	Tynagh lead-zinc deposit, Ireland	Intracontinental basin adjacent to active fault/exhalative	Lower Carboniferous, Upper Tournaisian-Lower Viscean	Sediment-hosted Pb-Zn-barite deposit; pyrite chimneys	Pyritised worm tubes	<100 m	(Banks, 1985; Little et al., 1998)
12	Ballynoe barite deposit, Silvermines, Ireland	Intracontinental basin adjacent to active fault/exhalative	Lower Carboniferous, late Tournaisian	Massive barite deposit (Sediment-hosted Pb-Zn associated)	Worm tubes, hematitised filaments	-	(Boyce et al., 2003)

13	Red Dog Zn-Pb- Ag deposit, western Brooks Range, Alaska, USA	Active horst & graben/ long-lived starved sedimentary basin	Carboniferous, Kuna Formation	Barites and sulfides hosted in siliceous black shale and chert; seep-related	Worm tubes, peloids	Offshore	(Moore et al., 1986; Campbell, 2006)
14	Canning Basin reefs, Western Australia	Platform margin to basinal/ post-depositional compaction, faulting	Upper Devonian, Frasnian, basinal facies, Gogo Fm.	Cool, early exhalative phase, stromatolite barite-sulfide build-ups	Intergrown stromatolites and barite	Deep basin	(Playford and Wallace, 2001)
15	Nikolaevskoe, Rudniy Altai, Kazakhstan	Ensialic island arc	Middle Devonian, Frasnian	VMS deposit	Worm tubes	-	(Avdonin and Sergeeva, 2020)
16	Oktyabrskoe, southern Ural Mountains, Russia	West Magnitogorsk island arc	Middle Devonian, Givetian, Karamalytash formation	VMS deposit	Worm tubes, brachiopods	>1400 m	(Maslennikov, 1991; Little et al., 1998; Maslennikov et al., 2017)
17	Barsuchiy Log, southern Ural Mountains, Russia	East Magnitogorsk island arc	Middle Devonian, Eifelian, Karamalytash formation	VMS deposit	Worm tubes	>1400 m	(Pshenichniy, 1984)
18	Gaiskoe, southern Ural Mountains, Russia	West Magnitogorsk island arc	Middle Devonian, Eifelian, Karamalytash formation	VMS deposit	Worm tubes	>1400 m	(Avdonin and Sergeeva, 2017)
19	Alexandrinka, southern Ural Mountains, Russia	East Magnitogorsk island arc	Middle Devonian, Givetian, Karamalytash formation	VMS deposit	Worm tubes in sulfide-barite layers; hematitised worm microtubes and filaments in gossanites	>1400 m	(Ayupova and Maslennikov, 2013; Ayupova et al., 2017; Maslennikov et al., 2017)

20	Molodezhnoe, southern Ural Mountains, Russia	East Magnitogorsk island arc	Middle Devonian, Givetian, Karamalytash formation	VMS deposit	Worm tubes, hematitised worm microtubes and filaments in gossanites	>1400 m	(Ayupova and Maslennikov, 2013; Maslennikov et al., 2016, 2017; Ayupova et al., 2017)
21	Priorskoe, southern Ural Mountains, Kazakhstan	Dombarovka back-arc basin	Middle Devonian, Givetian, Karamalytash formation	VMS deposit	Worm tubes, hematitised worm microtubes in gossanites	-	(Maslennikov et al., 2016, 2017; Ayupova et al., 2017)
22	Safyanovka, southern Ural Mountains, Russia	East Uralian Uplift (ensialic island arc)	Middle Devonian, Givetian	VMS deposit	Worm tubes, hematitised worm microtubes in jasper	>500 m	(Little et al., 1998; Ayupova and Maslennikov, 2013; Maslennikov et al., 2016, 2017; Ayupova et al., 2017)
23	Uzelga, southern Ural Mountains, Russia	East Magnitogorsk island arc	Middle Devonian, Givetian, Karamalytash formation	VMS deposit	Worm tubes, hematitised worm microtubes in gossanites	>1400 m	(Little et al., 1998; Ayupova et al., 2017; Maslennikov et al., 2017)
24	Talgan, southern Ural Mountains, Russia	East Magnitogorsk island arc	Middle Devonian, Givetian, Karamalytash formation	VMS deposit	Worm tubes; hematitised worm microtubes filaments and spherical bacterimorphic texture, hematite-quartz stromatolites in gossanites	>1400 m	(Ayupova and Maslennikov, 2013; Ayupova et al., 2017; Maslennikov et al., 2017)
25	Babaryk, southern Ural Mountains, Russia	East Magnitogorsk island arc	Middle Devonian, Givetian, Karamalytash formation	VMS deposit	Hematitised worm microtubes and filaments in gossanites	>1400 m	(Ayupova et al., 2017)
26	XIX Parts'ezd, southern Ural Mountains, Russia	East Magnitogorsk island arc	Middle Devonian, Givetian, Karamalytash formation	VMS deposit	Hematitised worm microtubes and filaments in gossanites	>1400 m	(Ayupova et al., 2017)
27	Uchaly, southern Ural Mountains, Russia	East Magnitogorsk island arc	Middle Devonian, Eifelian, Karamalytash formation	VMS deposit	Worm tubes, hematitised worm microtubes in gossanites	>1400 m	(Ayupova et al., 2017)

28	Sultanovka, southern Ural Mountains, Russia	East Uralian uplift (allochthonous fragments of evolved oceanic and epicontinental back-arc basin)	Middle Devonian, Givetian, Kasarga formation	VMS deposit	Worm tubes	-	(Maslennikov et al., 2016, 2017)
29	Sibay, southern Ural Mountains, Russia	Sibay intra-arc basin	Middle-Lower Devonian, Emsian-Eifelian, Karamalytash formation	VMS deposit	Annelid? worm tubes, *Tevidestus serriformis* (annelid worm tubes), *Sibaya ivanovi* (modiomorphid), indeterminate bivalves or brachiopods, hematitised worm microtubes in gossanites	Deep offshore, >1400 m	(Pshenichniy, 1984; Kuznetsov et al., 1988, 1991b, 1991a; Maslennikov, 1991; Little et al., 1997, 1999c; Shpanskaya et al., 1999; Campbell, 2006; Maslennikov et al., 2017, 2016; Ayupova et al., 2017; Georgieva et al., 2017)
30	Buribay, southern Ural Mountains, Russia	West Magnitogorsk island arc	Lower Devonian, Eifelian, Baimak-Buribay formation	VMS deposit	Worm tubes	>1400 m	(Little et al., 1998; Maslennikov et al., 2016, 2017)
31	Yubileynoe, southern Ural Mountains, Russia	West Magnitogorsk island arc	Lower Devonian, Eifelian, Baymak-Buribay formation	VMS deposit	Worm tubes, hematitised worm microtubes and filaments	>1400 m	(Little et al., 1998; Maslennikov et al., 2016, 2017; Ayupova et al., 2017)
32	Novo-Shemur, northern Ural Mountains, Russia	Tagil island arc	Silurian, Llandovery, Shemur formation	VMS deposit	Worm tubes, hematitised worm microtubes and filaments in gossanites	1400 ± 400 m	(Ayupova et al., 2017)

33	Shemur, northern Ural Mountains, Russia	Tagil island arc	Silurian, Llandovery, Shemur formation	VMS deposit	Hematitised microtubes and filaments in gossanites	1400 ± 400 m	(Ayupova and Maslennikov, 2013; Ayupova et al., 2017)
34	Komsomol'skoe, southern Ural Mountains, Russia	Sakmara marginal sea (Zaykov, 2006) or back-arc basin (Herrington et al., 2005c)	Silurian, Llandovery, Blyava formation	VMS deposit	Worm tubes	1400 ± 400 m	(Pshenichniy, 1984)
35	Blyava, southern Ural Mountains, Russia	Sakmara marginal sea (Zaykov, 2006) or back-arc basin (Herrington et al., 2005c)	Silurian, Llandovery, Blyava formation	VMS deposit	Worm tubes, hematitised microtubes and filaments in gossanites	1400 ± 400 m	(Ayupova and Maslennikov, 2013; Maslennikov et al., 2017)
36	Dergamysh, southern Ural Mountains, Russia	Main Uralian fault (supra-subduction zone)	Silurian	Co-Ni-bearing VMS deposit	Worm tubes	-	(Maslennikov et al., 2016, 2017)
37	Krasnogvardeyskoe, central Ural Mountains, Russia	Tagil island arc	Silurian, Llandovery, Krasnouralsk formation	VMS deposit	Worm tubes	1400 ± 400 m	(Ivanov, 1959; Little et al., 1998)
38	Ljeviha, central Ural Mountains, Russia	Tagil island arc	Silurian, Llandovery	VMS deposit	?Worm tubes, ?brachiopods	1400 ± 400 m	(Ivanov, 1959; Little et al., 1998)
39	Valentorka, central Ural Mountains, Russia	Tagil island arc	Silurian (or possibly Ordovician)	VMS deposit	Worm tubes	1400 ± 400 m	(Maslennikov et al., 2016, 2017)
40	Yaman Kasy, southern Ural Mountains, Russia	Sakmara marginal sea (Zaykov, 2006) or back-arc basin (Herrington et al., 2005c)	Silurian, Llandovery (or possibly Ordovician), Blyava formation	VMS deposit	*Eoalvinellodes annulatus* (indeterminate worm tubes), *Yamankasia rifeia* (indeterminate worm tubes), *Pyrodiscus lorrainae* (lingulid brachiopod), indeterminate	1600+ m	(Kuznetsov et al., 1993; Little et al., 1997, 1999c; Shpanskaya et al., 1999; Buschmann and Maslennikov, 2006; Campbell,

					lingulid brachiopod, *Mytilarca* (ambonychiid bivalve), *Thermoconus shadlunae* (monoplacophoran), indeterminate vetigastropod, indeterminate double-shelled fossil, hematitised worm microtubes, microbes and microbial biomarkers		2006; Blumenberg et al., 2012; Maslennikov et al., 2017, 2016; Ayupova et al., 2017; Georgieva et al., 2017, 2018)
41	Thalanga, Mt Windsor volcanic belt, northern Queensland, Australia	Back-arc basin/fault-associated brine-rich fluid flow	Ordovician, Trooper Creek Fm.	Sicila-iron exhalites in quartz-magnetite or hematite pods	Hematitic filament networks	Deep offshore, 1000+ m	(Duhig et al., 1992b, 1992a; Davison et al., 2001)
42	Løkken, area, Trondheim region, Norway	Back-arc basin	Lower Ordovician	Jaspers associated with VMS deposits	Hematitic filament networks	Deep offshore, 1000+ m	(Grenne and Slack, 2003; Little et al., 2004b)
43	Tally Pond belt, central Newfoundland, Canada	Rifted arc	Middle Cambrian	Metalliferous mudstones associated with VMS deposits	Worm tubes, sponge spicules	-	(Lode et al., 2016)
44	Niutitang Formation, Guizhou Province, western China	-	Lower Cambrian	Barite hydrothermal sedimentary deposit (SEDEX?)	Worm tubes, sponge spicules, algae	-	(Yang et al., 2008)
45	Gaobanhe Massive Sulfide, north China	-	Mesoproterozoic, 1.43 Ga	VMS deposit	Microbial fossils	-	(Li and Kusky, 2007)

46	Lady Loretta, Mt. Isa, McArthur River (HYC), northern Australia	Intracratonic basin/syn-depositional faulting	Paleoproterozoic, 1.64 Ga	SEDEX Zn-Pb-Ag deposits	Stromatolitic textures in pyrite, crinckly laminated filaments; biomarkers; b-Alkanes, squalane, isoprenoids	Shallow to deep water	(Oehler and Logan, 1977; McGoldrick, 1999; Logan et al., 2001)
47	Jerome district, Central Arizona, USA	-	Paleoproterozoic, 1.71-1.74 Ga	VMS-associated iron formation	Hematitic filament networks	Deep offshore, 850+ m	(Slack et al., 2007; Little et al., 2021)
48	Sulphur Springs, Pilbara Craton, Australia	Oceanic spreading centre	Paleoarchean, 3.23 Ga	VMS deposit	Pyritic filaments	Deep offshore, 1000+ m	(Rasmussen, 2000; Wacey et al., 2014)
49	Nuvvuagittuq belt, Quebec, Canada	-	Eoarchean-Hadean, 3.77-4.28 Ga	Iron formation	Hematitic filament networks	-	(Dodd et al., 2017)

1383

1384

Supplementary Materials

Figure S1. Searching for vent fossils in the field. **A**, open pit sulfide mine at Kambia, Cyprus, a location where vent fossils have been discovered. White areas on pit wall formed of gypsum, where exposed, potentially fossiliferous sulfides are currently being weathered. **B**, sulfide mine waste at Høydal, Norway, showing evidence of well-preserved sulfide textures considered highly prospective for fossil preservation. **C**, ore-horizon equivalent jaspers from Åmot Mine, Norway, along strike from Høydal that have yielded bacterial fossils (camera lens cap included for scale). **D**, sulfide block from Yaman Kasy mine, Russia, showing exceptionally well-preserved 'worm tube' fossils (pen included for scale).